

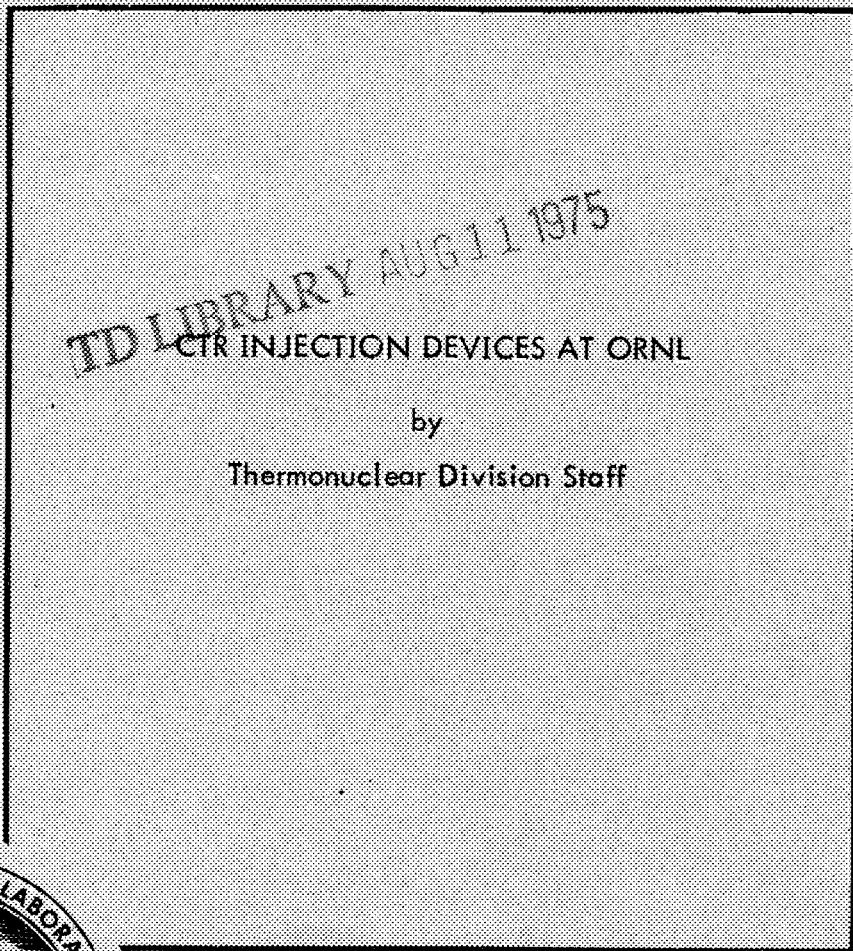
OAK RIDGE NATIONAL LABORATORY LIBRARIES



3 4456 0536792 9

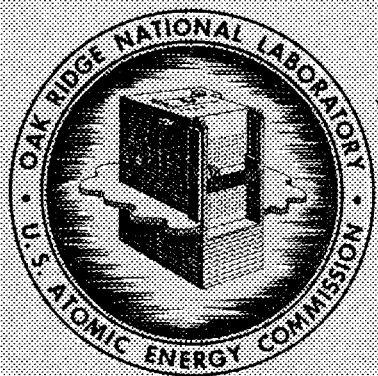
~~FOSTMA~~

ORNL-TD-67-1



TD LIBRARY AUG 11 1975
CTR INJECTION DEVICES AT ORNL

by
Thermonuclear Division Staff



OAK RIDGE NATIONAL LABORATORY
operated by
UNION CARBIDE CORPORATION
for the
U. S. ATOMIC ENERGY COMMISSION

TD-67-1

SPECIAL DISTRIBUTION

CTR INJECTION DEVICES AT ORNL

by

Thermonuclear Division Staff

July 1967

OAK RIDGE NATIONAL LABORATORY
Oak Ridge, Tennessee
Operated by
UNION CARBIDE CORPORATION
for the
U. S. ATOMIC ENERGY COMMISSION

PREFACE

This report has been prepared as a reference for the AEC Ad Hoc Panel on Plasma Confinement in Open-Ended Magnetic Configurations.

Members:

G. Bekefi	(MIT)	
A. S. Bishop	(AEC)	
H. Dreicer	(LASL)	
B. J. Eastlund	(AEC)	
T. K. Fowler	(GA)	Chairman
G. E. Guest	(ORNL)	
W. A. Perkins	(LRL)	
T. H. Stix	(PPPL)	
A. A. Ware	(AGN)	

CONTENTS

	PAGE
PREFACE	
1.0 INTRODUCTION	1
2.0 THEORY	2
3.0 PRESENT EXPERIMENTS	
3.1 DCX-2	3
3.2 DCX-1	13
3.3 DCX-1.5	24
3.4 INTEREM	29
4.0 IMMINENT EXPERIMENTS	
4.1 INTEREM + J	35
4.2 IMP	39
5.0 FUTURE EXPERIMENTS	45
TARGET PLASMA	
6.0 TECHNOLOGY	60
7.0 ECONOMICS IN OPEN-ENDED GEOMETRIES	61
8.0 APPENDICES	
8.1 Time Summary of ORNL Injection Experiments	64
8.2 Chart Summary of Parameters of ORNL Injection Experiments	65
8.3 Engineering Aspects of the IMP Magnet System	68
8.4 Detailed Time Schedule of the IMP Magnet System	79

1.0 INTRODUCTION

The purpose of this report is to present to the Ad Hoc Panel in as brief a manner as can convey information the salient features of the major ORNL low β open-ended confinement work. Brevity, charts, and outlines while concise have the disadvantage of understatement of the problems and their solutions. This method also leaves out much understanding of details which is relevant to simple statements made here in summary. With these obvious misgivings, we hope that this note is of some worth in the Panel's assessment of open-ended work. Further details of these experiments rest in the Chrestomathy, publications, and ORNL semiannuals, and we will be happy to supply details at any time.

2.0 THEORY

Since the codification of the pertinent instabilities is part of the function of the Ad Hoc Panel and since Gareth Guest is undertaking this as a primary assignment, it would be premature and redundant to include that as a part of this report. Thus we have here concentrated on the experimental parameters and results. Though we have compared these results to the appropriate instabilities, we have not attempted to rank the instabilities as to their ultimate importance.

3.1 DCX-2

3.1.1 Introduction

This summary has three objectives:

- (1) to review the essential features of the DCX-2 device
- (2) to discuss the results of the experiments
- (3) to indicate directions of future experiments.

3.1.2 General Description

The magnetic field and physical design of the DCX-2 facility is shown in Figs. 1 and 2. Operating parameters are indicated below:

A. Injection parameters

1. Molecular ion injection at 540 keV
2. Beam currents up to 70 mA maximum
3. Fractional dissociation (F):

$$F = 1 - e^{-n\sigma_D L} \text{ where dissociation cross section}$$

$$\sigma_D = 1.2 \times 10^{-16} \text{ cm}^2$$

L = total path length of beam

n = density of dissociating centers

(a) Gas dissociation: L \sim 50 meters
 $F \approx 1.8 \times 10^{-2}$ for $p_0 \sim 10^{-6}$ torr

(b) Arc dissociation: for arc diameter of 3 cm,
 density 3×10^{13} ions/cm³.

$F \approx 10^{-2}$ for each pass of beam through arc. For

L \approx 50 m, 50 beam transits can be expected and total fractional dissociation \sim 0.40. As high as 0.70 has been observed under some arc conditions.

B. Operating pressures

1. Base pressure $\sim 5 \times 10^{-8}$ torr
2. Arc dissociation $\gtrsim 10^{-6}$ torr
3. Gas dissociation $10^{-7} - 5 \times 10^{-5}$ torr

C. Magnetic field

1. Field details are shown in Figure 1.
2. The field can be made uniform ($\sim .1\%$) over volume two feet diameter and 4.5 feet in length.

3.1.3 Plasma Properties

Upon dissociation, the injected proton distribution is a delta function in perpendicular energy (270 keV) and axial velocity ($E_{\parallel} = 1.6$ keV), and is expected to be unstable to ion gyrofrequency instabilities. Continuous ion cyclotron harmonic signals are observed throughout the injection interval. The distribution is strongly modified in times ~ 10 msec to an equilibrium plasma consisting of three main components:

A. Central peak plasma

1. Contains most of the trapped density up to $n = 5 \times 10^9$ ions/cm³ with arc dissociation; up to $n \sim 10^8$ ions/cm³ with gas dissociation.
2. $T_{\parallel} \sim 500$ eV peaked at $E = 0$.
3. Large spread in T_{\perp} (15 keV $< T_{\perp} >$ 3 MeV) with mean $E_{\perp} \sim 700 - 800$ keV.
4. Plasma dimensions: $\bar{R} \sim 15 - 25$ cm, $L \sim 100 - 150$ cm
Chamber wall radius 45 cm.
5. Confined in central magnetic field region where $\Delta B \sim 10 - 20$ gauss. Thus, mirror ratio ~ 1.001 .
6. $T_{\perp}/T_{\parallel} > 10^3$ highly anisotropic with $R/a \sim 3$, $L/a \sim 20$

B. Side lobe plasma

1. Contains $< 10\%$ of central peak density.
2. Retains injected axial energy. ($E_{\parallel} \approx 1-2$ keV with $\Delta E_{\parallel}/E_{\parallel}$ as large as 0.4 under some conditions.)
3. $T_{\perp} \sim 150$ keV
4. Plasma dimensions: $R \approx 15$ cm, $L \sim 3$ meters, limited radially by injector duct.
5. $T_{\perp}/T_{\parallel} < 10^2$ with $R/a \sim 3$, $L/a \sim 70$.

C. Background plasma

1. Arc dissociation:
 - (a) Plasma density not well established but density generally exceeds energetic ion density by at least a factor of ten.
 - (b) $T_i \approx 100$ eV; $T_e \approx \phi \left. \begin{array}{l} \\ \end{array} \right\} < 50$ eV
 - (c) Fills entire available volume with radial profile like energetic ion profile.
2. Gas dissociation:
 - (a) Plasma density varies with pressure: at $p \sim 10^{-6}$ torr $n_e \approx n_{+}(\text{hot})$
 - (b) Electron energy varies with pressure: at $p \approx 10^{-7}$ torr $T_e \approx 300$ eV, $\phi \sim 1$ keV.
 - (c) Ion energy < 50 eV.

D. Review of General Features. DCX-2 has many features making making it ideal to compare experiments with theoretical models to answer stability criteria questions.

1. It contains a dense energetic plasma with $\omega_{pi,hot} \sim \omega_{ci}$.
2. It approximates the usual assumptions of uniform field infinite medium calculations. Field uniform to .1% over volume 10 - 35 Larmor radii long.
3. The energetic ion distribution is measureable and reproducible as functions of $v_{||}$, v_{\perp} , radial position, and time through ~ 40 diagnostic ports.

3.1.4 Objectives

The objectives of the experiments are the observation and understanding of the properties of the following general classes of instabilities:

- A. Ion-electron loss-cone modes. The general threshold is given by $\omega_{pe} > \omega_{ci}$ or $n_e > 5 \times 10^6$ electrons/cm³. These thresholds are modified slightly when taking into account finite radius and length (e.g., G. E. Guest and R. A. Dory)¹.
- B. Ion-ion flute-like modes or loss-cone modes. General criterion is that $\omega_{pi,total} > \omega_{ci}$ or $n_+ > 6.6 \times 10^9$ ions/cm³. These instability thresholds depend on (n_c/n_H) as shown by Budwine, Farr, and Guest², but the present operating regime with arc dissociation just reaches the density region of interest. An energetic ion density increase of a factor of 3 - 10 is desirable to insure exceeding thresholds which may be set by the finite plasma size.

Handwritten notes:

$$n = 6 \times 10^9 \text{ ions/cm}^3$$

$$\left(\frac{n_c}{n_H} \right) = \frac{6 \times 10^9}{10^9} = 6$$

3.1.5 Results

Experiments so far have concentrated on detailed observations of Class A instabilities (the ion-electron modes).

- A. Observations were made during the "afterglow", i.e., after the beam is stopped, in gas dissociation. The plasma produced by gas dissociation was observed to decay stably, with decay times ~ 100 msec, at densities $\sim 10^8$ ions/cm³. The predicted threshold for this instability is $\sim 1 - 2 \times 10^7$ particles/cm³, but detailed study of the dispersion relation by Beasley, Guest, and Dory³, inspired by this observation, led to the conclusion that the instability is convective for $n < 5 \times 10^8$ particles/cm³ and absolute above this density. An alternative explanation of the observed stability, Landau damping by warm electrons, is excluded since electrons of ~ 1 keV temperature is required. Under the experimental conditions, $T_e \sim 50$ eV.

The observation of the absolute growth of the instability is prevented in gas dissociation by the density limitation. With arc dissociation, however, ion-cyclotron radiation is observed, in bursts, in the afterglow for densities above $\sim 5 \times 10^8$ ions/cm³. Before a proper assignment of the instability mode can be made, however, detailed measurements of the plasma distribution and, especially, the background plasma properties, must be established. Efforts in this direction are in progress.

- B. A study of the ion-electron gyrofrequency instability in the annular cylindrical plasma defined by the molecular ion beam has been carried out. For these studies, the trapped energetic proton plasma was depressed by obstacles placed suitably or,

alternatively, by using a helium injected beam. No arc was used. Two propagating waves were identified, $k_{\parallel} v_{\parallel}^{(\text{beam})} > 0$ (convective) and $k_{\parallel} v_{\parallel}^{(\text{beam})} < 0$ (absolute). The predicted thresholds $\omega_{pe} = 2\omega_{ci}$ were verified for the first two harmonics. The modes predicted in the model of Burt and Harris (and observed in an electron experiment by Morse) would propagate with shorter wavelengths than actually observed. These short wavelength modes, however, are expected to be Landau damped by the electrons with observed $T_e \approx 30$ eV. In fact, the wavelengths observed corresponding to previously unstudied modes of the dispersion relation, are the minimum consistent with Landau damping by the electrons. For the observed instabilities, for all the observed harmonics, $v_{\text{phase}} \approx 4 v_e$.

The non-linear limit of the instability has also been established. The measured electric fields are consistent with the total available charge taking part in the fundamental instability mode. There is no evidence that higher harmonics are driven by the non-linear behavior — the second harmonic, for example, grows linearly at its predicted threshold and possesses a different wavelength than the first harmonic.

3.1.6 Future Plans

The present planning for the DCX-2 device is divided into two phases: (1) attaining improved densities so as to encompass all the expected instability regimes, and (2) study of the instability properties.

A. Improved densities

The objectives are to improve the density in the central peak plasma while limiting the density in the side lobe plasma to present levels.

Present studies are designed to test the scaling of the plasma lifetime and the density as a function of beam current. The available results are not yet definitive. Density rises with injection current, although probably not linearly. The losses from the central peak plasma can be accounted for by charge exchange. The experiments are however not definitive and alternative description cannot be ruled out. A detailed accountability of injected particles has not yet been carried out since only an unknown fraction ($\sim 10\%$) of the dissociated protons are trapped in the central peak plasma. Experimental studies designed to separate the injection rate into the central peak plasma from the loss rate are presently in progress.

B. Instability studies

Multiple probe arrays are to be used for direct measurements of axial and azimuthal wavelengths of the observed instabilities in the afterglow of plasmas produced by arc dissociation. An assignment of the observed instability will be based on a comparison of the observed k_{\parallel} , n_c/n_{Hot} and n_{Hot} with the predictions of Budwine, Farr, and Guest² on the multiple component ion-ion instability and those of Dory, and Beasley³ on the ion-electron modes.

Either assignment is possible from the present evidence.

Other studies of the radio frequency behavior shortly after beam turn-on ($t \ll \tau_{\text{cx}}$) may indicate the instability mode responsible for the creation of the observed equilibrium plasma. These studies are a natural sequel to the results obtained from the investigation of the instability in the molecular ion beam.

C. Specific experiments

The main objectives of the DCX-2 program are to use the central peak plasma to test instability theories and to increase the central peak density so instabilities can be studied at higher densities. Secondary aims are the study of the origin of the central peak plasma, the equilibrium properties of the hot ion plasma and the mild microinstability of the injected beam. Future experiments that relate to these objectives are listed below.

1. Completion of the test of the scaling law $N_+ V = I_{inj} F \tau$ now in progress.
2. Extension of the magnetic field to permit added stage of differential pumping for use with hydrogen arc to allow lower operative pressures in central field region (expect pressure reduction of factor ~ 10).
3. Continue study of molecular ion beam instability. Determine reason for observed k_{\parallel} , investigate growth of convective mode and attempt to assess reflection at end of plasma. Establish to what extent these effects may be extrapolatable to other convective ion-electron modes.
4. Determination of which of the two instabilities, Harris mode or multi-group flute-like mode, is responsible for the rf observed after beam turnoff with hydrogen arc dissociation. This involves accurate time-resolved measurement of the cold plasma density after beam turnoff, since the instability thresholds as the multi-group mode depend on the cold ion density. The hot ion density and velocity distribution function will be obtained at times

just preceding the occurrence of rf bursts during plasma decay to obtain quantitative comparison with theory. Measurement of the axial instability wavelength and signal polarization should help to decide between the two instabilities.

5. Study of the formation of the central peak plasma at early times after beam turn-on to determine the trapping into the central peak group and the relevant loss process.
6. Study of the parameter changes which cause the transition from a dominant central peak group to a dominant side lobe group with gas dissociation.

3.1.7 References

1. G. E. Guest and R. A. Dory, Phys. Fluids 8, 1853 (1965).
2. R. E. Budwine and W. M. Farr, Bulletin of APS Series II, Vol. 12, No. 5, 1967, p. 629.
3. C. O. Beasley and R. A. Dory, TED Semiannual Report, ORNL 3989, April 30, 1966.

3.2 DCX-1

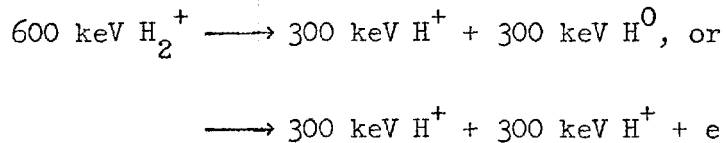
Experiments in the DCX-1 facility began in 1957 and were terminated in 1966, when the field coils and main vacuum vessel were used for DCX-1.5. The facility was used for technological development and plasma study.

3.2.1 Machine Description

- 1.1 The magnet field configuration was a simple 2:1 mirror, with $B_0 \approx 10$ kilogauss and mirrors at $Z \approx \pm 15$ inches. The coil and diagnostic arrangements permitted plasma radii of 8 to 10 inches with axial extents up to ± 6 inches.
- 1.2 Plasma was formed by dissociation of 600 keV H_2^+ in this trap. The injected H_2^+ currents were initially measured in microamperes, and were later gradually increased to a maximum of about 15 mA. The injection trajectory was confined to the median plane and made but a single pass through the trap. The trajectory was arranged so that its closest approach to the magnetic axis was tangent to the circular midplane orbit for 300 keV H^+ ($R = 3.25$ in.). When arcs were employed, they were operated along field lines so as to intersect the H_2^+ beam at this tangent point.
- 1.3 Base (operating) pressures were initially $\sim 1 \times 10^{-6}$ torr, gradually decreased to $\sim 1 \times 10^{-9}$ torr.

3.2.2 Dissociation Mechanisms, Trapping Fractions(F), and Plasma Distributions

Fast proton input to the trap was obtained by dissociation of a fraction of the H_2^+ beam:



We define the trapping fraction (F) as the ratio of proton input current to H_2^+ beam current. Three distinctively different dissociation mechanisms were employed. Here they are described in chronological order.

2.1 The initial emphasis (1958 - 1960) was on carbon arc dissociation, with the arc operated in the geometry described in paragraph 1.2. With such localized dissociation, the protons were essentially all introduced on nearly circular orbits, so the distribution of injected protons was ring-like (minor diameter ~ 2 in.), centered about the magnetic axis. F was a function of arc properties, and for the usual arc currents (≈ 300 amperes) ranged from 4 to 40%. However, certain properties of the arc which could not be overcome severely limited the lifetime of the trapped protons: partially stripped carbon ions rather than ambient neutrals dominated charge-exchange losses; and the sea of cold arc electrons ($\sim 10^{13} \text{ cm}^{-3}$, ~ 5 eV) rapidly reduced trapped proton energy ($-dE/dt$ order of 10 keV/msec). Since in the vicinity of 300 keV, the cross-sections for charge-exchange loss of protons vary like E^{-4} , the energy degradation resulted in much higher charge-exchange loss rates. Even so, the highest fast proton densities obtained in DCX-1 were those with carbon arc dissociation ($\approx 5 \times 10^9 \text{ cm}^{-3}$, from

$n^+ = IF\tau/v$ with $I = 5 \text{ mA H}_2^+$, $F = 4\%$, $\tau = 6 \text{ msec}$, and $v = 1\ell$).

Plasma lifetimes scaled approximately as F^{-1} , so the changes in arc properties that varied F from 4 - 40% resulted in approximately the same hot ion densities.

The fact that at low pressures essentially all loss of hot ions occurred by charge exchange with the arc itself negated the initial emphasis placed upon the possibility of obtaining burnout in these experiments. Burnout was the process by which the hot ion plasma would virtually eliminate neutral gas from the plasma interior by ionization. If the rate of ionization ($n^+ n_0 \sigma_i v_+ V$) of neutral gas within the plasma could be made greater than the rate at which neutrals entered ($\frac{n_0 v A}{4}$), burnout would occur. The neutral density within the plasma would decrease, and the charge-exchange lifetime and hence hot ion density would increase proportionally, leading to an even greater rate of ionization, further reduction of neutral density, etc. Assuming only loss by charge exchange on background neutrals, it was estimated that a critical ($I_{\text{H}_2^+} F$) product of about 8 mA would suffice for burnout of a neutral background of 1×10^{-7} torr. However, as pointed out above, charge-exchange losses in the arc itself were completely dominating at such pressures.

Dissociation on hydrogen gas arcs was briefly investigated in attempts to develop an arc that did not contribute much to hot

ion loss. However, we were not able to produce gas arcs that would permit operation at pressures lower than 1×10^{-5} torr, and gas dissociation (below) dominated trapping.

2.2 The emphasis then turned to gas dissociation on ambient gas neutrals (1961 - 1963). Here

$$n^+ = \frac{IF\tau}{V} = \frac{I(n_0 \sigma_d^0 L)}{V(n_0 \sigma_{cx} v_+)} = \frac{I \sigma_d^0 L}{V \sigma_{cx} v_+},$$

hence F is much smaller and with otherwise constant parameters n^+ is independent of pressure. The trapping collisions were distributed along the H_2^+ beam trajectory, so the plasma distribution was smeared out, though still peaked at the circular orbit radius. The volume of initially injected plasma was 2 - 4 liters. At low pressures instability-driven scattering resulted in larger equilibrium volumes and diluted the central proton density (peak density) to about 1/3 that expected on the basis of the initial volume figure.

Without arcs, the environment was much more conducive to detailed plasma studies, and this interval saw the development of most of our critical diagnostics for measurements of charge-exchange loss fluxes, plasma potential, energy distribution, low frequency electrostatic signals, and high frequency electrostatic and magnetic signals. There was also considerable effort placed on reducing the ambient neutral pressure in hopes of obtaining

exponentiation of plasma density through dissociation of H_2^+ on plasma already trapped. This trapping term was omitted in the equation above. Its inclusion results in:

$$n^+(t) = \frac{I(n_0 \sigma_d^0 L)}{V(\frac{1}{\tau'})} \left(1 - e^{-t/\tau'} \right)$$

where

$$\frac{1}{\tau'} = \left[(n_0 \sigma_{cx} v_+) - \frac{I \sigma_d^+ L}{V} \right],$$

so with $I \tau_{cx} > V / \sigma_d^+ L$, a stable plasma would build up to scattering limited density. The expression, which does not include burnout effects, is valid at low n_0 ($P = 10^{-8} - 10^{-9}$ torr). At high n_0 the inclusion of burnout significantly reduces the critical $I \tau$ product, but in doing so requires I very much greater than was available. At low n_0 the burnout effects are negligible. Hence the omission of this term and the emphasis upon low ambient neutral pressure.

From the last equation we estimated the critical $I \tau$ product to be ~ 500 mA sec, but though ~ 300 mA sec was achieved (corresponding to a hot ion density $\sim 1 \times 10^8 \text{ cm}^{-3}$), we did not see evidence of exponentiation, at least partly because of instability effects (Section 3.2).

2.3 Later experiments employed Lorentz dissociation of injected H_2^+ (beginning in 1963). Here one uses the $\underline{v} \times \underline{B}$ force acting on H_2^+ ions in the trap to dissociate those in upper vibrational levels. To obtain an H_2^+ beam rich in such levels (H_2^{+*}), it was necessary to extract H_3^+ from the ion source and to create H_2^{+*} from this in a water vapor cell. The end result was a low current beam (maximum of 1 mA) for which a fraction $F = (1 - 2) \times 10^{-4}$ could be Lorentz dissociated in the DCX-1 trap. With pressures low enough to yield $\tau_{cx} > 1$ sec, $n_0 \sigma_d L < 1 \times 10^{-4}$, and the trapping was predominantly Lorentz. At lower pressures the trapping was essentially all Lorentz, so there $F = (1 - 2) \times 10^{-4}$, independent of n_0 , and without exponentiation

$$n + \approx \frac{I(10^{-4}) \tau_{cx}}{V}$$

for stable plasma. The exponentiation condition (Section 2.2) is not changed; again, no evidence of exponentiation was observed.

A trapping fraction of 10^{-4} is admittedly small, but with $\tau > 1$ sec, Lorentz dissociation of the 1 mA H_2^{+*} beam produced greater proton input than could be obtained with gas dissociation of the full 15 mA of directly extracted H_2^+ current. During these experiments, τ 's of tens of seconds were routinely available and without instability densities of $5 \times 10^9 \text{ cm}^{-3}$ should have accumulated. The injected plasma radial distribution, as with gas

dissociation, was smeared by the distributed nature of the dissociation interactions. The equilibrium densities were reduced by instability-driven scattering to larger volume, as before, and under some conditions (Section 3.2) by direct loss of protons.

3.2.3 Instability Studies

- 3.1 No detailed instability studies were made using arc dissociation. Comparisons of proton input currents with charge-exchange loss currents indicated that charge-exchange losses dominated any direct instability losses. Flute stability could have resulted from line tying by the arc. Energy spread of trapped protons was large, $\sim 100 - 200$ keV full width at half maximum, with spreads mostly toward energies less than the injected energy but with significant extent at higher energies. It did not appear that diffusion by coulomb collisions could account for the latter; fluctuating rf fields in the arc and possibly in the hot plasma itself were apparently involved. Also it was noted that the energy loss rate of trapped protons increased with hot ion density for fixed arc properties, another probable indication of hot ion instability. In view of later observations (below) it is probable that the plasma had microinstabilities.
- 3.2 Essentially the same instability phenomena were observed with gas as with Lorentz dissociation. The greatest distinction between these situations was that the higher proton input currents available with Lorentz trapping permitted observation of hot ion losses driven directly by microinstability.

Low frequency hot-ion instability (flutes) were not observed.

That the growing "unstable" flute mode was absent is understandable -- the analysis of Kuo, et al.,¹ indicates threshold at $\sim 5 \times 10^8 \text{ cm}^{-3}$ for DCX-1, and the microinstability limited density was lower ($\sim 2 \times 10^8 \text{ cm}^{-3}$). It is surprising that "stable" flute modes were not seen, and we have no ready explanation for this fact.

High-frequency (microinstability) modes were present. We observed:

- a. "Z mode" oscillations, present at pressures of 10^{-8} torr and below, weak at electrostatic probes and strong at magnetic probes arranged for sensitivity to current fluctuations along z. The threshold hot ion density was $\lesssim 5 \times 10^6 \text{ cm}^{-3}$. This instability was responsible for burst-like ejections of plasma electrons out along field lines and consequently kilovolt fluctuations of plasma potential. It did not drive fast proton losses and had only a minor effect on scattering protons to volume larger than that associated with the injection and trapping process. It could be damped completely with very small amounts (fractions of a watt) of electron cyclotron heating. The observed frequencies were not proton cyclotron harmonics, but rather of the form $(n\omega_{ci} \pm \omega_z)$ where ω_z was the

¹L. G. Kuo, E. G. Murphy, M. Petravac, and D. R. Sweetman, Phys. Fluids 7, 988 (1964).

proton axial oscillation frequency (the Z betatron frequency). This frequency distribution prompted an explanation in terms of a Harris-like mode with the frequency of the ion oscillator Doppler shifted by axial oscillation at ω_z . One supposes that the quenching of this instability by electron cyclotron heating was the result of Landau damping, but this point was not unambiguously demonstrated.

- b. " θ -mode" oscillations at $n\omega_{ci}$, present at all pressures, strong at both electrostatic probes and magnetic probes oriented for sensitivity to θ current fluctuations. These are most effective at scattering protons to larger volume, at spreading their energy distribution, and at driving direct losses of protons. The instability was shown to be negative mass by a series of self consistent experiments which yielded quantitative agreement with theory. The experiments included measuring the response of threshold to changes in (1) magnetic field shape, (2) energy spread of trapped protons, and (3) proton distribution in radial oscillation amplitude; and dependence of fundamental mode frequency on changes in radial oscillation amplitude.

The detailed studies of this instability showed that the stability properties of the usual plasma distribution were those of a toroidal core centered on the circular midplane proton orbit and containing only a few percent of the population of the entire usual distribution. Lowest thresholds ($\sim 4 \times 10^5 \text{ cm}^{-3}$)

occurred when the toroidal distribution was well ordered, as was the case for the usual plasma distribution. With Lorentz dissociation, the instability drove direct losses which were first detected at $5 - 10 \times 10^7 \text{ cm}^{-3}$; these losses accounted for as much as 0.9 of the proton input current to the plasma; and, along with instability-driven scattering to larger plasma volume, they limited the proton density to $1 - 2 \times 10^8 \text{ cm}^{-3}$, as much as a factor of 15 below the density expected in the absence of such effects. With gas dissociation at low pressures, instability-driven scattering and lower proton injection current resulted in maximum densities less than the threshold for observation of direct losses with Lorentz dissociation, and instability losses were negligible.

Reducing the order of the central toroidal distribution (as with deliberately introduced energy spread or shift of H_2^+ trajectory) had a pronounced effect on instability threshold, and could in fact increase threshold density by factors up to about 40. However, the instability limited density increased only by about 2 x.

- c. A second variety of θ -mode oscillation, observed only at low pressures with the high densities available with Lorentz trapping. The threshold hot ion density was $\sim (5 - 10) \times 10^7 \text{ cm}^{-3}$. RF signals were $1 - 2 \text{ MH}_z$ below gyrofrequency, leading to the

designation diminished frequency mode. The mode was intermittent, but when present also drove direct proton losses. The instability was not identified with any theoretical model.

3.3 DCX-1.5

The DCX-1.5 facility was commissioned in mid-1966 (calendar) and continues operation at the present time. As indicated below, it serves not only as a tool for plasma research but also as a proving site for technological development required in anticipation of the IMP facility. The latter will use the injection system of DCX-1.5 but a more complex field geometry. Experiments with the DCX-1.5 configuration are to be terminated in late 1967.

3.3.1 Machine Description

- 1.1 Magnetic field configuration is the simple 2:1 mirror of DCX-1, but is sometimes powered up to $B_0 = 14$ kilogauss.
- 1.2 Plasma is formed by Lorentz ionization of an injected energetic H^0 beam, usually 15 keV. Most of the trapping is from the states with principal quantum number $N \approx 15$. $F = 1.5 \times 10^{-4}$ (see Section 3.3.2.2).
- 1.3 The beam line consists of a duoplasmatron source for 30 keV H_2^+ , a conversion cell usually charged with magnesium but sometimes barium, plus drift spaces and collimating apertures for differential pumping sections.
- 1.4 The injection trajectory is in the median plane and passes through the magnetic axis.
- 1.5 The beam burial section is at present rudimentary but surprisingly effective. The beam leaves the plasma region through a single aperture and impinges upon a water-cooled titanium plate in a cavity which is also supplied with titanium-getter pumping.

1.6 The main vacuum vessel and research area are those of the DCX-1 facility.

3.3.2 Technological Development

- 2.1 Maximum injected beams have been 44 mA (equivalent) of 15 keV H^0 through the last defining aperture, 1.5 in. diameter at 96 in. from the conversion cell. Beams of 25 - 30 mA are routinely available.
- 2.2 Conversion of H_2^+ to H^0 has been tested in both magnesium and barium neutralizer cells. With each we find that highest proton input current to the trap is obtained with "thick" cells. These produce $I^0/I_{H_2^+}$ ratios of about 1.8 and trapping fractions (referenced to I^0) of $\sim 1.5 \times 10^{-4}$. The latter implies fractional excited state populations which scale like $0.5/N^3$. The scale factor (0.5) is not particularly sensitive to conversion cell thickness. Tests of vapor-jet neutralizers are now in progress.
- 2.3 Best trapped proton lifetimes have been 160 msec, equivalent to charge-exchange loss on a hydrogen background (molecular) of $\sim 1.5 \times 10^{-9}$ torr. These lifetimes were obtained with an 8 mA H^0 beam and were reduced to ~ 60 msec with change to an 18 mA beam. Typical values for operation with 20 - 30 mA H^0 are 20 - 50 msec.
- 2.4 Deliberate introduction of energy spread by rapid modulation of the duoplasmatron extractor potential (i.e., H_2^+ beam energy) has

produced trapped proton energy distributions with measured spreads of 55% full width at half maximum.

- 2.5 Development (with Tennelec Instrument Co.) of a surface barrier detector and preamplifier system for energy analysis of charge-exchange neutrals. The low energy detection limit is 6 keV, and the resolution (at 10 keV) is 2.8 keV full width at half maximum.

3.3.3 Plasma Properties

- 3.1 Two microinstabilities are observed. One, which we term the Z mode, is associated with axial current fluctuations. The other, the θ mode, is associated with azimuthal current fluctuations. Signals from the Z mode occur in a band 5 - 7 MHz wide about $2\omega_{ci}$. θ mode signals are at $n\omega_{ci}$. In addition there are both stable and unstable flute oscillations.
- 3.2 The Z and the stable flute modes have low density thresholds (order 10^6 hot ions/cm³) and do not drive observable proton losses. The modes are generally suppressed at higher densities (10^7 cm⁻³ range) by transition to the θ or to the unstable flute mode. Transition to either of these modes establishes an instability limit on further plasma accumulation.
- 3.3 The θ instability is suppressed by operation at high magnetic field ($B_0 \gtrsim 12.5$ kilogauss). With both θ and unstable flute modes suppressed, the Z and stable flute modes remain. Plasma confinement is limited by charge-exchange losses up to a density at least

$n^+ \approx 4 \times 10^8 \text{ cm}^{-3}$, the highest value permitted so far by the available beam at base operating pressure.

- 3.4 The unstable flute is suppressed by operation with grounded end walls close to the hot ion region ($Z = 1.5$ to 3 in.). The observed threshold density for the unstable flute as a function of end wall location relative to the median plane is in reasonable quantitative agreement with the recent "line tying" theory of Guest and Beasley.¹ For this agreement, it is necessary to take the dielectric constant of the cold plasma regions linking hot ions with the end plates as that of a vacuum. Since the Debye length in the cold plasma regions is probably \gtrsim the length of these regions, the assumption appears to be reasonable.

3.3.4 Future Work

4.1 Technological

- a. Tests of water vapor jets for beam neutralization, with evaluations of conversion efficiency, relative excited state populations, and gas streaming load into the hot plasma region. Also tests of multiple neutralizing jets in different potential regions as a means of producing energy spread in the injected H^0 beam.
- b. Work to increase the actual injected H^0 current up to 100 mA, the test stand performance for the present source.
- c. Measurements of trapping fractions (indirectly, the relative excited state populations) with proton rather than H_2^+ beams

¹G. E. Guest and C. O. Beasley, Phys. Fluids 9, 1798 (1966).

incident upon magnesium, barium, and possibly water vapor jet neutralizing cells.

- d. Possibly, tests of a liquid helium cryopump.

4.2 Plasma Studies

- a. Continuation of flute stabilization studies, with addition of plasma potential determinations, cold plasma probes, and some extension of flute theory.
- b. Measurement of threshold properties of the microinstabilities, to include effects of electron cyclotron heating at low power levels (watts).

3.4 INTEREM

The Interem facility was developed to investigate the accumulation of energetic ions in a large volume simple mirror by charge exchange trapping of injected energetic neutral atoms with cold ions produced in an ECH (electron cyclotron heated) plasma. Two aspects of the problem must be separated -- (1) the generation of a suitable ECH plasma, and (2) the study of the accumulated energetic ion plasma. Both aspects have been investigated in the Interem facility.

3.4.1 Machine Parameters

A. Magnetic field:

- | | | | |
|-------------------------------------|---|------------------|----------|
| 1. <u>Simple mirror</u> | { | 3:1 mirror ratio | (Fig. 1) |
| | | 2:1 mirror ratio | |
| 2. <u>Extended multiple mirrors</u> | | | (Fig. 2) |

B. Injected beam:

Up to 100 ma of H^0 at 20 kev in a beam < 2" diameter

C. Microwave power:

Up to 50 kW at 10.6 GHz (3-cm wavelength)

3.4.2 Motivations

A. ECH plasma:

1. Simple mirrors:

The initial experiments in the simple 3:1 mirror were designed to establish the properties of the ECH plasma in a scaled up (10 x Volume) version of the PTF facility. The results showed the

equilibrium plasma to consist of three components:

- a. "Cold" electrons $n_e \simeq 5 \times 10^{11} \text{ e/cm}^3$ $T_e < 100 \text{ ev}$
- b. Warm electrons $n_e \simeq 5 \times 10^{11} \text{ e/cm}^3$ $T_e = 120 \text{ kev}$
- c. Hot electron tail $n_e < 10^{10} \text{ e/cm}^3$ $E > 2.2 \text{ Mev}$

A minimum pressure was required, $\sim 8 \times 10^{-6}$ torr, for macro-stability at maximum power.

2. Extended mirrors:

The objective of these experiments was to improve the ratio of electron density to neutral density in the center of the ECH plasma by producing ECH plasma outside the main mirror regions where the ambient pressure and, therefore, particle influx may be high. Power applied to the central volume was to aid in heating and trapping of the ECH plasma drifting in from the ends. Although the electron density is still too low, the added length of the plasma permits operation of macro-stable ECH plasmas at ambient pressures as low as 4×10^{-6} torr with 49 kW applied power. Under these conditions the plasma consists of the following properties:

$$\begin{array}{ll} n_e(\text{cold}) \simeq 10^{11} \text{ e/cm}^3 & T_e \leq 100 \text{ ev} \\ n_e(\text{warm}) \simeq 10^{11} \text{ e/cm}^3 & T_e \sim 100 \text{ kev} \\ n_e(\text{hot}) \sim 10^{10} \text{ e/cm}^3 & E > 2.2 \text{ Mev} \end{array}$$

The lower electron densities in the extended field case is directly attributable to the low power density. Results of the beam injection experiments clearly show the electron density increased with power, but failure of some of the klystron amplifiers limit the available power, at present, to $< 25 \text{ kW}$.

B. Injected energetic ion plasma:

The objective, stated simply, is to accumulate the maximum possible density of 20 keV ions through the efficient charge exchange trapping of the injected, neutral beam. Guideposts which relate to interesting densities are set by instability thresholds. The instabilities of concern are as follows:

1. Precessional $\nabla B/B$ drift instability:

a. Absence of cold plasma. Assuming no cold plasma present, the threshold has been given by Kuo, et al., as

$$n = 3.9 \times 10^5 \left(\frac{\nabla B}{r_0 B} T_i \right) = 10^7 \text{ ions/cm}^3$$

for T_i = ion energy in eV and for $\frac{\nabla B}{B} = 1.6 \times 10^{-2} \text{ cm}^{-1}$ and $r_0 = 15 \text{ cm}$.

b. Cold plasma present. Using the results of Guest and Beasley,¹ taking into account finite length of the hot plasma and the presence of a dense electron component, Interem is stable against precessional drift modes at all ion densities except for probably unimportant narrow resonances,

2. Ion-electron instabilities:

As indicated previously, instabilities may be expected for

$\omega_{pe} = l\omega_{ci}$. However, with $T_e = 10^5$ volts, all such gyrofrequency modes up to at least $l \sim 25$ may be expected to be Landau damped.

3. Ion-ion multiple component modes:

According to present calculations, ω_{ci} instabilities of these modes should be present for $n_c/n_H \approx 10^2 - 10^3$ but only at high

¹G. E. Guest and C. O. Beasley Phys Fluids 9, 1798 (1966).

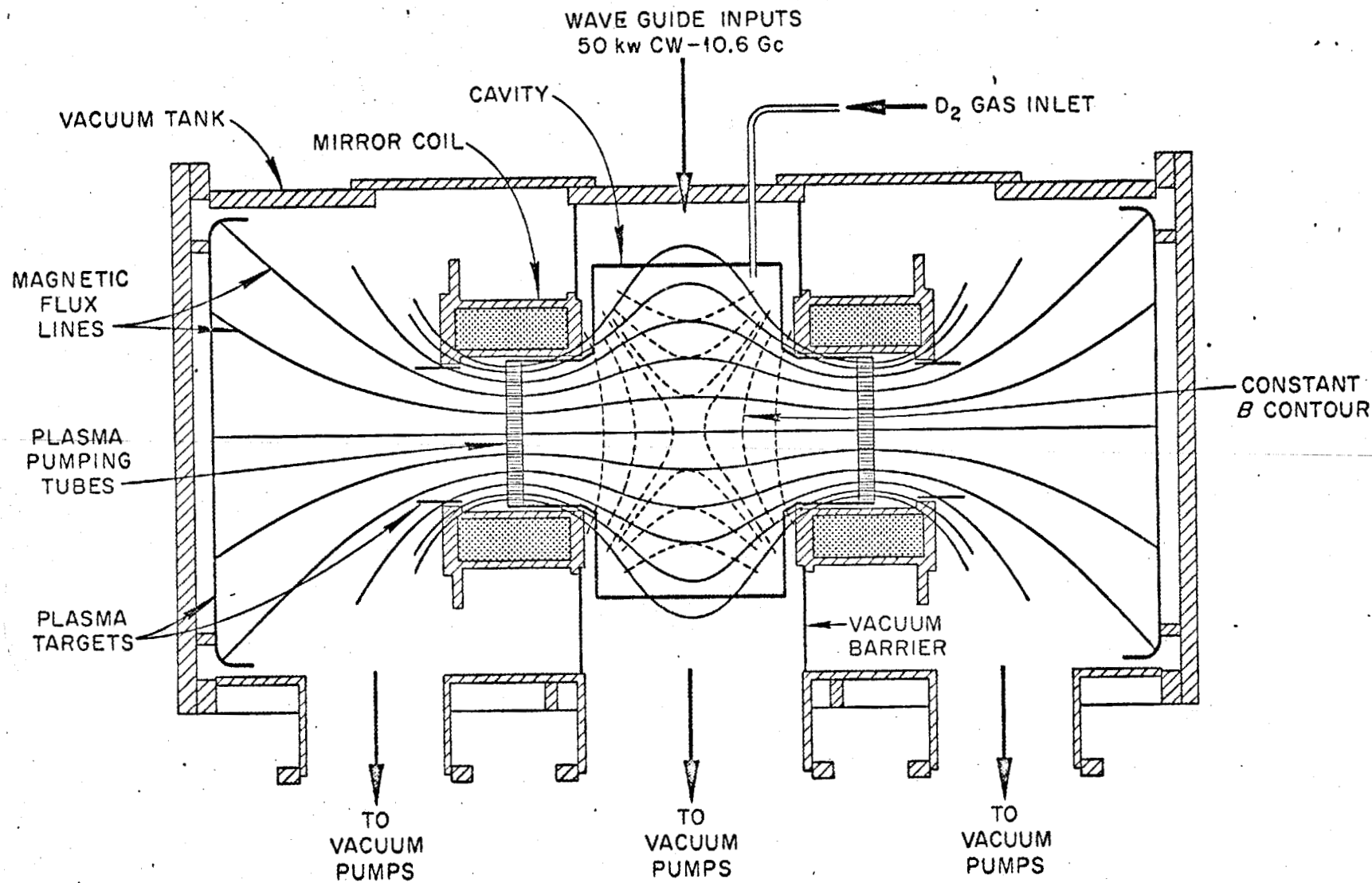
harmonics ($l \gtrsim 20$). It is not clear that the effect of such instabilities would be detectable in the present experiments, i.e., the expected wavelengths are so short that the energy change or volume spreads may be too small to be detectable. To date, radio frequency signals in the expected frequency range ($\sim 20 \omega_{ci}$) have not been studied.

3.4.3 Results

A gross (and, perhaps, overgeneralized) outline of the results of the study of the ECH plasma was given in Section 3.4.2A. All the energetic ion plasma properties have not yet been measured in detail. However, for the beams of ~ 100 ma so far injected, the density has reached $\sim 5 \times 10^8$ ions/cm³. No gross evidence for instability can be seen, i.e., low harmonic ion gyrofrequency signals do not exist, axial plasma spread is not discernible, and the density is observed to increase linearly with beam current. The density improvement over gas dissociation at a given pressure is consistent with the known cross-sections.

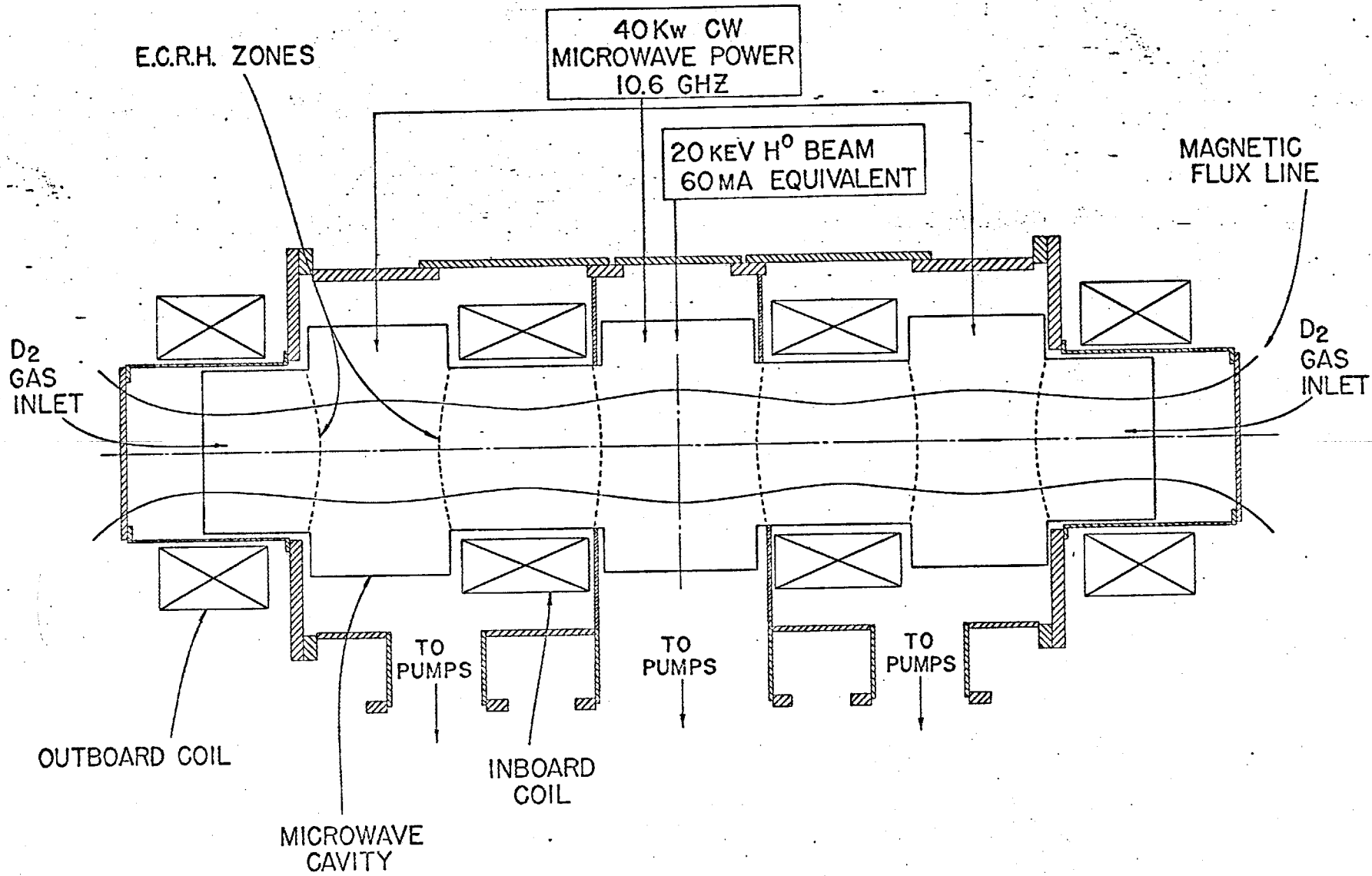
3.4.4. Future Plans

The present series of experiments are being terminated and the extended magnetic mirrors are being removed to investigate the energetic ion plasma in 2:1 mirror configuration but with higher microwave power density. Time will permit only cursory measurements to be carried out in order to allow the installation of the quadrupole coils described in Section 4.1. In view of the time limitations, the motivations are basically technological, and will vary parameters appropriate to target plasmas, but should interesting deviations from natural behavior be detected these general statements will require revision.



33

FIG. 1 INTEREM (SIMPLE MIRROR)



E.P.A.
ELECTRON-CYCLOTRON RESONANT HEATING EXPERIMENT
WITH ENERGETIC NEUTRAL INJECTION

FIGURE 2

4.1 INTEREM WITH QUADRUPOLE MIN-B FIELD

4.1.1 Rationale

The desiderata of injecting energetic ions into a target plasma of hot electrons have been discussed in the Chrestomathy and seem to be fairly well established. It was pointed out, however, that to generate a "successful" hot ion plasma in this way, the required target density is $\sim 3 \times 10^{13}$ particles/cm³ in an ambient pressure below 10^{-6} torr. These requirements have not yet been met by ECH plasmas in simple mirror fields, in part, at least, because as the ambient pressure is reduced, low frequency fluctuations are strongly evident and the plasma becomes macroscopically unstable. This phenomenon has been related to the absence of a sufficient density of cold plasma at the low pressures to achieve the necessary "line tying" for stability of the intermediate energy electron population.

In order to establish the greatest chance of success for generation of a suitable target plasma, it is thought that a min-B configuration should be provided. With a sufficiently deep well, general considerations indicate that low frequency (μ -conserving) instability modes should be suppressed, thus permitting operation at the lowest ambient pressures consistent with sufficient particle throughput to produce an equilibrium state.

Experimental evidence is available to support these stability arguments, although it should be recognized there still exists a large gap between the experiments and quantitative theoretical predictions. Certainly, the most ideal comparisons are available from hot ion injection devices such as ALICE, PHOENIX, and DCX 1.5, where $\nabla B/B$ precessional drift instabilities have been

unequivocally demonstrated to result in stable or unstable identifiable oscillations and plasma loss. When multipole fields are added to the simple mirrors, these oscillations are completely absent. Experiments using pulsed plasma injection have also observed strong fluctuations which were related to plasma losses which were suppressed by sufficiently deep magnetic wells, but the specific instability modes in the various cases are not yet unambiguously established. Typical of these experiments are those of Ioffe and the devices MTSE, DECA, and Toytotop. The experiments by Hartman in min-B geometries, in which ECH plasmas were used, also noted the effectiveness of the well for stabilization, but the characteristics of the plasma are somewhat different from that desired for the target plasma in that $T_e \lesssim 3$ kev. However, it is not yet clear that Hartman's experiments include the specific regime of ECH plasmas which is needed for a target plasma.

4.1.2 Machine Design Parameters

The Interem facility will be modified as shown in Fig. 1. The quadrupole coils, wound with copper already on hand, will require 1.5 MW to produce the range of well depths desired. The wall mirror ratio in the midplane is 1.5 and may be varied by adjustment of the quadrupole current down to a simple mirror configuration. The $|B|$ contour, 3780 gauss, on which electrons resonate with the applied microwave frequency has been chosen, nominally, to a radius midway between the axis and the wall, as shown, but may be varied continuously to a point on axis or to the wall radius. Resonance off the midplane occurs closer to the axis so that the resonant surfaces take the spatial form of a slightly distorted football. The location of the microwave

waveguides are chosen to take advantage of the field flexibility without leading to arcing in the guides.

4.1.3 Objectives

The experimental program is still in a somewhat empirical form and must remain so until the kinds of plasmas which can be produced are established. The objective will be to determine the properties of the ECH plasma and to establish the effectiveness of the min-B geometry in reducing the cold electron component relative to the hot electron population. The emphasis will be on establishing the means by which the electron temperature and distribution function may be placed in the hands of the experimenter. When suitable hot electron plasmas are developed, neutral injection will be used to establish an energetic ion plasma and to measure ratio of electron density to neutral pressure on the axis, a parameter essential to the continuation of target plasma trapping.

Planning beyond this is dependent on the relative success in attaining these first objectives, but our current thoughts include modification of the field (by the redesign of the present coil configuration) so that available 1.7 cm μ -wave power may be applied. Under these circumstances, the density of the ECH plasma should increase sufficiently that we will have at least 5 - 6 ionization mean free paths for thermal neutrals incident on the hot electron plasma surface. This attenuation will permit observations on the degree of residual neutral density remaining from fast protons resulting from dissociation of ionized molecular hydrogen (Frank Condon neutrals), and should result in considerable higher accumulated ion densities.

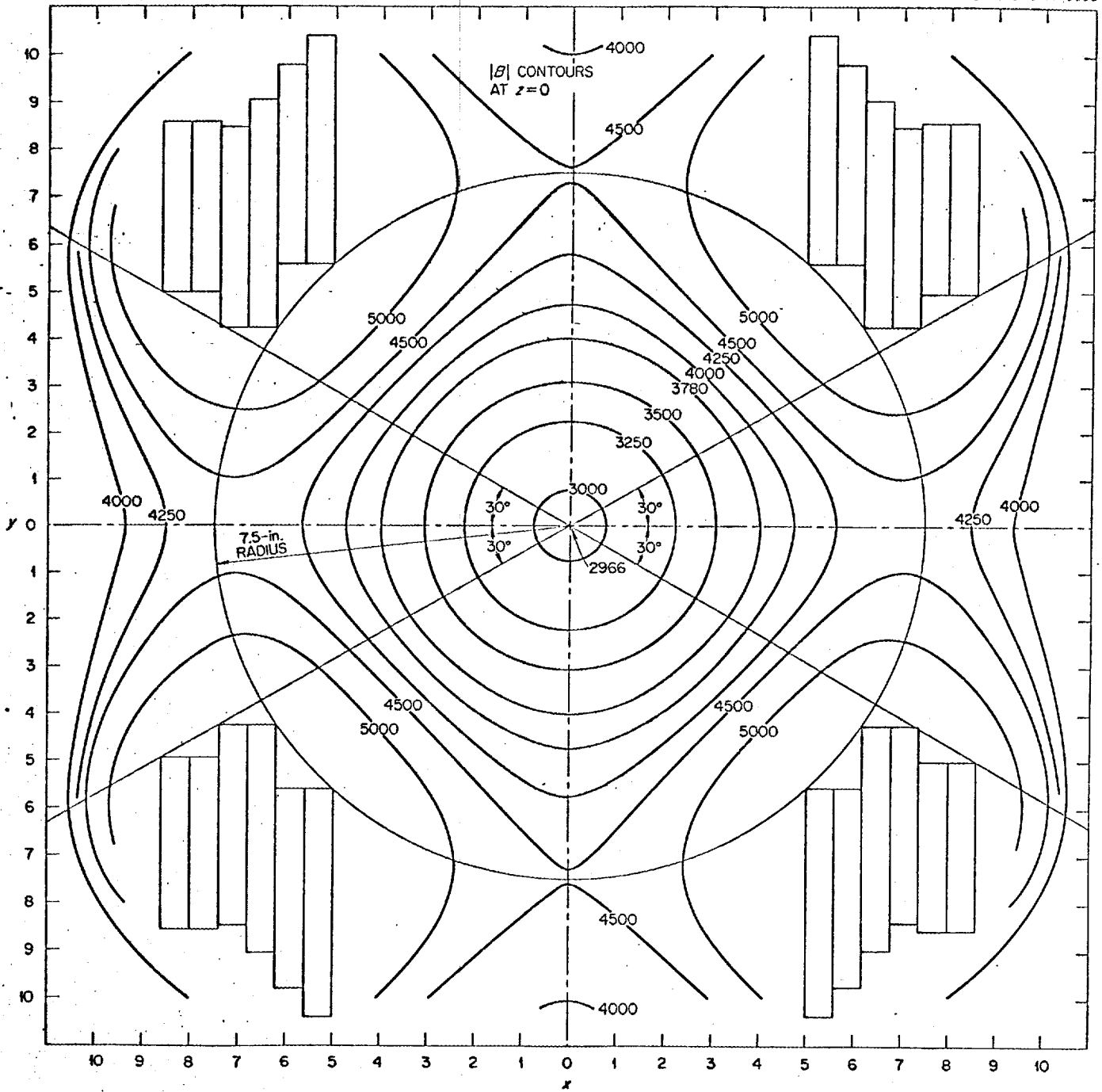


FIGURE 1 MOD-B SURFACE FOR INTEREM + J

4.2 IMP

4.2.1 General Description

The IMP (Injection into Microwave Plasma) facility, now in an advanced design stage, will establish a hot proton plasma by ionization of 20 keV H^0 injected into a magnetic well trap. The injector, diagnostic systems, and research site and controls, will be those presently in use with the DCX-1.5 facility. The trap, which is the major new item, will be of the mirror plus quadrupole variety and will establish a Phoenix II-like field through steady state superconducting coils rather than pulsed. Base operating pressures in 10^{-10} torr range are expected.

The device has three objectives of varying difficulty and promise for achievement:

1. Injection of 20 keV neutral beam into a mirror-quadrupole magnetic field in which trapping is by Lorentz ionization and control of instabilities is through energy spread and electron cyclotron heating.
2. Studies of ECH. This facility can be used to a limited degree to generate an electron cyclotron plasma for regions appropriate to 8 mm and 5.5 mm heating in a min -B geometry, to test the scaling and suitability for a "target plasma".
3. Injection into ECP
 - A. The intriguing possibility of operating with ambient pressure at low values so that electrons resulting from Lorentz ionization of fast neutral beam is the dominate feed for the ECP must be tested as a possible trapping and stability control mechanism.
 - B. Injection into a dense ECP if objective 2 is achieved is of interest since efficient trapping and additional stability control is possible. This serves as a limited "proving ground" for the more ambitious target plasma.

4.2.2 Machine Description

1. Design: IMP is a multi-purpose min -B facility, thus some of the features listed below will not be suitable for all the anticipated uses.

2. Machine Parameters:

A. Neutral Beam:

In general the neutral beam is existing equipment with proven results and though refinements are being made and are desirable we feel what we have is good for the immediate objectives.

1. Energy - the energy is variable from 10 - 50 kev though most experiments will be done at 20 kev.
2. Intensity - we have obtained 60 ma (equiv) of 40 at 20 kev and are attempting to duplicate the 100 ma obtained by Kelley and Morgan on a test stand in an equivalent geometry (1.5" ϕ at 90").
3. Conversion Cell - we have used magnesium and barium. Other metal vapor cells will be tested.
4. Trapping
 - a. Lorentz Trapping is main trapping in low pressure regime. Trapping is from $n = 10, 11$.
 - b. Cascading - Inverted cascading can populate states suitable for trapping if density is in the range for collisional excitation ($n_e > 10^9$).
 - c. Charge Exchange Trapping - Trapping (as in Interem) by charge exchange of hot H^0 on cold H^+ is effective for $n_{\text{cold}} > 10^{10}$ and is most likely when ECP is established.
5. Beam Dump - a simple beam dump (as in DCX 1.5) will be employed initially though room is left for a more elaborate facility should it be warranted.

6. Energy Spread - energy spreads of 55% FWHM have been obtained.

B. Vacuum

Because of the vast helium surfaces in the tank cryopumping (4.2°k) is present and pressures $< 10^{-10}$ torr are anticipated. Our experience at $10^{-10} - 10^{-9}$ torr range in DCX-1 and DCX-1.5 shows that such pressures are not unreasonable.

C. Magnetic Field

The principal new hardware item which is the main design problem is the superconducting mirror plus quadrupole min -B well. Because IMP is a facility capable of several experiments, the flexibility of separate controls of mirrors and quadrupoles was thought to be mandatory.

The details are given in Sections 8.3 and 8.4 but a summary is included here for completeness:

1. $B_0 = 20$ kilogauss with a 2:1 axial mirror ratio and closed modulus B contours up to 26 kilogauss (for $B_0 = 20$ kg).
2. Superconducting wire is NbTi (.080 × .080 cross section) which has been tested to carry 535 amps in 75 kilogauss. Coil design figures are for < 450 amps.
3. Experimental access is appreciated by examination of the figures in 8.3.
4. Construction schedule indicates the completion of mirror trap in October 67 and of the well in Jan. 68.

D. Microwave Power

Available for use at various stages of experimentation is the following microwave power:

1. 8 mm Resonant with 12 kg we have tubes of 50 w, 200 w, and 2 kw.

2. 5.5 mm Resonant with 19 kw we have tubes of 100 w, 1 kw, 5.5 kw, and in August 67, 16 kw.

4.2.3 Experimental Rationale

A. INJECTION EXPERIMENTS

IMP will be primarily devoted to detailed study of microinstabilities relevant to the target plasma program. To be emphasized are:

1. Effects of Landau damping of cyclotron modes with $k_{\parallel} \neq 0$. These experiments will use the plasma established by Lorentz ionization at low pressure with control of T_e by ECH at 8 mm and at 5.5 mm. Hot ion densities in the $10^9 - 10^{10} \text{ cm}^{-3}$ should be available so $\omega_{pe}/\omega_{ci} \geq 30$.
2. Properties of the "double-humped" instability as functions of n_c/n_H , total $\omega_{pi}^2/\omega_{ci}^2$, and the energy spread in the hot ion distribution. We look first at the possibility of controlling n_c and total ω_{pi}^2 by heating electrons to a point at which their mirror confinement time equals the hot ion confinement time. Any further incremental increase of T_e could then cause trapping of cold ions by reversal of the positive potential well established by normal ambipolar processes.

The Lorentz-trapped distribution is an excellent one for such studies, since both hot ion density and electron feed are initially independent of electron-cyclotron heating rate. One can create an electron cyclotron heated component at low microwave power. Thus the situation should allow more control of the desired parameters than available in present experiments. If it is possible to produce and control electrostatic confinement of cold ions by mirror confinement of electrons, one thus could increase cold ion density

to enhance the trapping rate for fast neutrals (by cascading and charge exchange trapping).

Other more common parameters which are at the experimenter's control are: well depth, energy spread, spatial spread, modification of radial distribution through preionization, and others mentioned earlier in this section.

B. Electron Cyclotron Heating

Another group of experiments which do not employ injection of neutrals will be the investigations of the creation, heating, and confinement of a dense electron plasma in a min -B configuration. This is a part of the studies necessary to establish the target plasma.

Like the experiments to be done with 3 cm ECH in the INTEREM + J facility, the IMP will be used to measure density, temperature, and confinement properties of 5.5 mm ECP established in a min -B well. It will be necessary to establish scaling before embarking on a more ambitious target plasma.

Necessarily these studies would be investigations of high β plasmas in a min -B geometry. Experiments in Elmo have already demonstrated that 60% β is attainable in a configuration stabilized by line-tying. In IMP we would extend such investigations to plasmas established in shallow min -B to replace the line tying stability and thus the "throughput". We can then even deepen the well by the use of high β hot electron plasmas and thus have a deep well available for additional stability for ions.

C. Target Plasma

Should the 5.5 mm ECP possess the electron density and temperature suitable for trapping and stability, IMP would inject neutrals into the ECP and investigate the initial target plasma concept in the min

-B. Such questions about the ultimate target plasma such as trapping, attenuation of ambient gas pressure, stability, could be experimentally assessed for the low power ECP.

4.2.4 Summary

We have presented the physical characteristics, parameter control, and motivation for the IMP facility. It is apparent that IMP will extend the Phoenix, Alice Baseball, and AGN experiments to exercise control over the electron temperature and density.

In addition IMP will provide a study vehicle to assess the trapping and stability of a target plasma created by low power microwave heating.

5.0 Future Experiments (Target Plasma)

One emphasis at ORNL has been the progression toward a Target Plasma Experiment. This has been apparent throughout this report in the rationale of many aspects of IMP and in the total dedication of the INTEREM experiments. What the final plasma suitable for a target plasma will be rests upon the experiment proof of several assertions.

We have in a general way outlined the Target Plasma Program objectives, philosophy, and benchmarks in an ORNL-4080 report which is reproduced here as the major part of this Section.

We will be more specific in a proposal to be given to the committee in a later document.

5.0 ORNL TARGET PLASMA PROGRAM

R. A. Dandl

G. E. Guest

N. H. Lazar

ABSTRACT

In this report we enumerate some of the considerations underlying a proposed program for accumulating a dense energetic-ion plasma in an open-ended magnetic well by injecting fast neutral atoms into a target plasma produced by electron-cyclotron resonant heating. The report gives a brief discussion of the plasma stability problems, emphasizing those aspects which bear on the target plasma program, and a summary of the known characteristics of electron-cyclotron heating. Trapping efficiency is illustrated by a detailed buildup calculation, included as an appendix. A tentative timetable showing the anticipated evolution of the program is given.

INTRODUCTION

The central objective of present controlled-fusion experiments using injection and trapping of energetic particles in open-ended magnetic traps is the production of a stable energetic-ion plasma of sufficient density to permit an evaluation of the ultimate loss rate of energetic ions from the trap. This objective has not yet been achieved, primarily because of the occurrence of a variety of plasma instabilities which strongly affect the plasma confinement. Considerable progress has been made toward understanding the causes of many of these instabilities and in devising suitable stabilization techniques. We discuss this question separately in the section "Stability Considerations." At this point we shall only summarize the main features of the stability problem as it relates to open-ended configurations, first as regards the sources of instability and then as regards the available stabilization techniques.

All confined plasmas may reduce their energy by expansion, so that open-ended as well as closed systems share this common reservoir of free energy, that is, energy available to drive growing oscillations. However, if the expansion is the result of low-frequency fluctuating electric fields ($\omega \ll \omega_{ci}$, the ion gyrofrequency), it is not energetically possible in a magnetic well.

It is also recognized that because of the loss cone, characteristic of open-ended traps, complete thermalization is not possible. The associated energy reservoir can drive a number of growing high-frequency oscillations which need not be constrained by the magnetic well. Fortunately, many of these waves propagate at least partially along the magnetic field and thus are subject to electron Landau damping. The importance of this constraint is greatly enhanced in an open-ended trap, since the finite length of the plasma limits the axial wavelength (hence the axial phase velocity as well), making possible the realization of the condition for Landau damping:

$$\omega/k_{\parallel} \lesssim 3V_{\text{thermal}}$$

This same finite-length feature of open-ended configurations also makes possible an electrical "short circuit" of incipient charge clumps, provided that the electrical communication with conducting end plates is effective.

The two free-energy reservoirs mentioned above, due to confinement and the nonthermal character associated with the loss cone, are unavoidable consequences of confinement in open-ended traps. The injection of energetic particles can, however, lead to additional departures from thermal equilibrium in the form of trapped distinct groups of high-energy ions. Post has suggested a scheme of programmed injection in which the degree of thermalization arising from Coulomb scattering will at all times in the accumulation stage be sufficient to avoid velocity-space instabilities (by elevating the necessary threshold densities above the instantaneous value of the density). This scheme relies heavily on achieving extremely low pressures of ambient gas in order to have scattering rates exceed charge-exchange rates and anticipates buildup times of seconds, during which times the plasma is vulnerable even to comparatively weak instabilities.

In the present note we shall advance an alternative proposal which seeks to utilize the much more rapid accumulation possible in an environmental plasma, where the trapping processes — charge exchange and ionization by electron impact — are roughly three orders of magnitude more efficient than the Lorentz-force trapping which must be relied upon at low pressures. Rather than seek to eliminate the energy reservoir associated with injection of fast particles, we hope to exploit the strong stabilizing constraints available in open-ended traps: magnetic well configurations, strong Landau damping, and electrical "short circuiting" through conducting end walls. In the following section, we shall give a general outline of the technological problems and present status of electron cyclotron plasmas, returning to the stability problem in the section "Stability Considerations."

THE TARGET PLASMA

We next consider the technology associated with the production of a target plasma which can provide efficient trapping of injected fast atoms and rapid accumulation of the resulting fast ions. Since 1960 a number of experiments have been carried out at ORNL using steady-state microwave power at a frequency corresponding to the electron gyrofrequency on some surface within the confining magnetic field ("heating zones"). For most of the experiments the magnetic field was a simple mirror trap, but more recent experiments have used multiple mirrors (INTEREM) and the "folded cusp" (ELMO) configurations. We first review the results obtained in simple mirror traps.

A dominant feature of these plasmas is the cold-plasma stabilization of low- β interchange instabilities, since the necessity of maintaining a minimal cold-plasma density limits the range of stable operation to ambient gas pressures in excess of around 10^{-5} torr. The most fundamental problem arising from this high-density neutral-gas environment is the flux of nonthermal neutrals, resulting from dissociation of H_2^+ and charge exchange of warm ions, which penetrate the plasma region and seriously reduce the lifetimes of the trapped fast ions. In addition, much of the applied microwave power may be required for throughput of cold plasma, since the average lifetime

of cold ($T_e \sim 50$ to 100 eV) plasma is usually less than $100 \mu\text{sec}$. Some experiments at 35 Gc/sec have shown an encouraging departure from this trend, however, in that most of the electrons reached a temperature of ~ 3 keV, with much less power required for cold-plasma throughput. We shall consider this difficult question of power scaling in more detail later.

One other recognized stability property has influenced the choice of operating parameters in the past, namely, that if the heating zones fell too close to the midplane, instabilities, tentatively identified as mirror instabilities, were generated. It was inferred from these observations that the anisotropy of the energetic electrons was increased as the heating zones approached the midplane until the instability threshold, $T_{\parallel}/T_{\perp} \lesssim \beta$, was crossed. In practice, this mode has been easily avoided by suitable location of heating zones.

In brief, then, in a simple mirror trap and within limits set by interchange and mirror stabilization criteria, one can produce a plasma of energetic electrons and cold ions of density such that $\omega_{pe} \sim \frac{1}{2}\omega$ microwave. Experience to date has suggested that the necessary specific power is around $\frac{1}{2}$ to 2 W/cm³, although this figure depends sensitively on the type of energy distribution produced as well as the plasma density. The distribution of electrons in energy depends on the experimental parameters in a complex way which is only partially understood, so that power requirements, especially in other types of traps, remain an open question.

Since few generalizations seem justified at present, we shall tabulate some illustrative experimental cases in Table 1.

As yet only a few experiments have been carried out in the magnetic well geometry produced by the folded-cusp fields in ELMO, shown schematically in Fig. 1; and no attempts have yet been made to create steady-state electron-cyclotron-heated plasmas in Ioffe-type traps or "baseball" geometries.

Because of present uncertainties in the folded-cusp geometry, apparently related to the null in the magnetic field, and because of the necessity of producing the target plasma in a magnetic well, experiments are being initiated whose objective will be the production of an electron-cyclo-

Table 1. Summary of Electron-Cyclotron Plasma Operating Parameters

Facility	Microwave Frequency, ν_0 (Gc/sec)	Density of Electrons			Volume (liters)	Power (kW)	Ambient Gas Pressure (torrs)	Mirror Ratio
		Hot $\langle N_e \rangle_H$	Intermediate $\langle N_e \rangle_I$	Cold $\langle N_e \rangle_c$				
PTF	10.6	$\lesssim 10^9$ (> 2 MeV)	$\sim 5 \times 10^{11}$ (70 keV)	$\lesssim 10^{10}$ (~ 100 eV)	2 to 5	2 to 5	$> 1 \times 10^{-5}$	2:1
INTEREM	10.6	$\lesssim 10^9$ (> 2 MeV)	4 to 7×10^{11} (120 keV)	$\lesssim 10^{10}$ (~ 100 eV)	30	40	1×10^{-5}	3:1
ELMO	.35	Absent	$\lesssim 10^{11}$ (50 keV)	2 to 5×10^{12} (3 keV)	$\lesssim 1$	1.8	1×10^{-5}	1.7:1

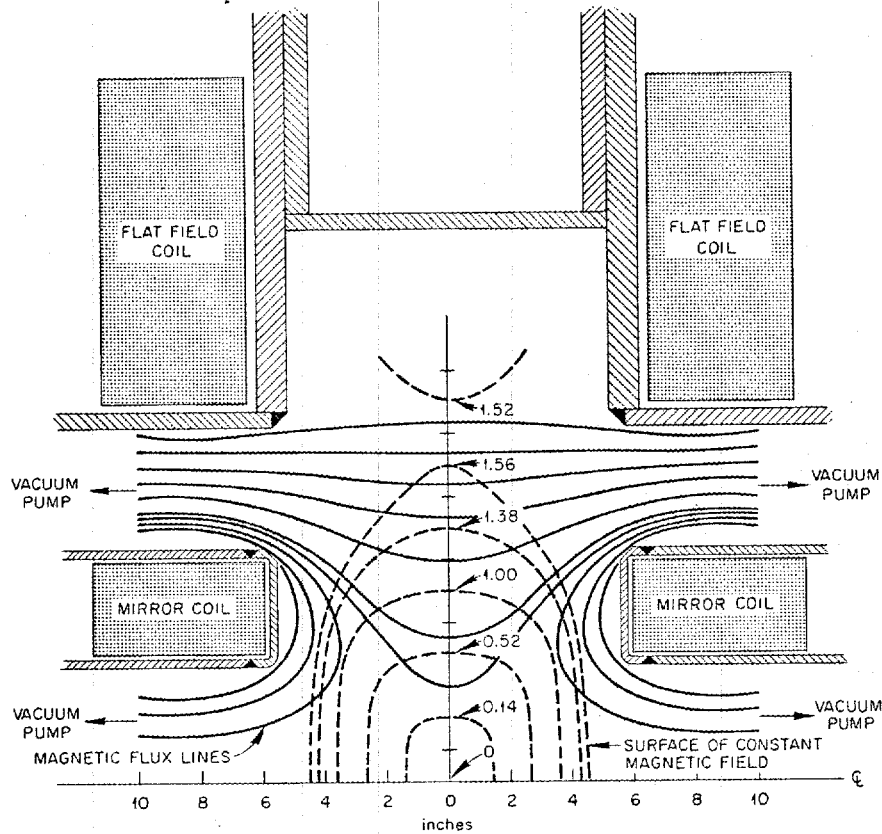


Fig. 1. ELMO Schematic. Folded cusp configuration.

tron-heated plasma in a Ioffe-type trap. Present plans are to modify the existing INTEREM field by adding (quadrupole) Ioffe bars. This configuration does not have a null, but power limitations restrict the well depth to smaller values than in the folded cusp. In initial experiments a well depth $\Delta B/B \sim \frac{1}{2}$ is expected. It is hoped to demonstrate the feasibility of electron-cyclotron heating with the 3-cm microwave power presently available and to study power scaling laws with 1.7-cm microwave power, which should be available soon.

It remains to specify the density and volume of the target plasma toward which our program must develop. We attach an illustrative buildup calculation, which, although admittedly and deliberately pessimistic, shows the possibility of obtaining $>10^{12}$ ions/cm³ at 20 keV by injecting a few tenths of an ampere of neutral atoms into a target plasma of $>10^{13}$ electrons/cm³ with ambient gas pressures of 10^{-6} torr. The plasma volume was taken to be around 4 liters. If, as was suggested above, the electron density is limited by $\omega_{pe} \sim \frac{1}{2} \omega$ microwave, then the assumed target-plasma density can only be realized by using microwave power at 5.5 mm (54.6 Gc/sec). This, in turn, implies 20-kG magnetic field strengths for the trap.

It is not possible to specify the total amount of microwave power necessary to produce this target plasma, since one of the major power-loss mechanisms in mirror traps, cold-plasma throughput, should no longer be important in magnetic well geometries. However, if Coulomb scattering becomes the dominant loss mechanism, then required specific power levels should vary as

$$\frac{\text{power}}{\text{volume}} \approx \frac{\omega_{pe}^4}{25.8 \log_{10} R} \frac{\ln \Lambda}{\left(\frac{m^3}{\pi k T_e}\right)^{1/2}}$$

Or, if $\omega_{pe} \sim \frac{1}{2} \omega_{\text{microwave}} = \pi \nu_0$,

$$\frac{\text{power}}{\text{volume}} \sim 4\nu_0^4 \frac{\ln \Lambda}{\log_{10} R} \left(\frac{m^3}{\pi k T_e}\right)^{1/2}$$

Thus for $T_e \sim 10$ keV, $\nu_0 = 54.6$ Gc/sec, and $\ln \Lambda / \log_{10} R \sim 45$,

$$\frac{\text{power}}{\text{volume}} \sim \frac{20 \text{ W}}{\text{cm}^3}$$

In order to allow for various uncertainties, we shall request 100-kW capabilities at 5.5 mm wavelength.

We include a tentative timetable (Fig. 2) listing the major programmatic developments leading to the full-scale experiment outlined above. Present injection experiments in the INTEREM facility are expected to continue for approximately six months (A). Design improvements in the injection system are expected to lead to currents in excess of 200 mA and resulting trapped ion

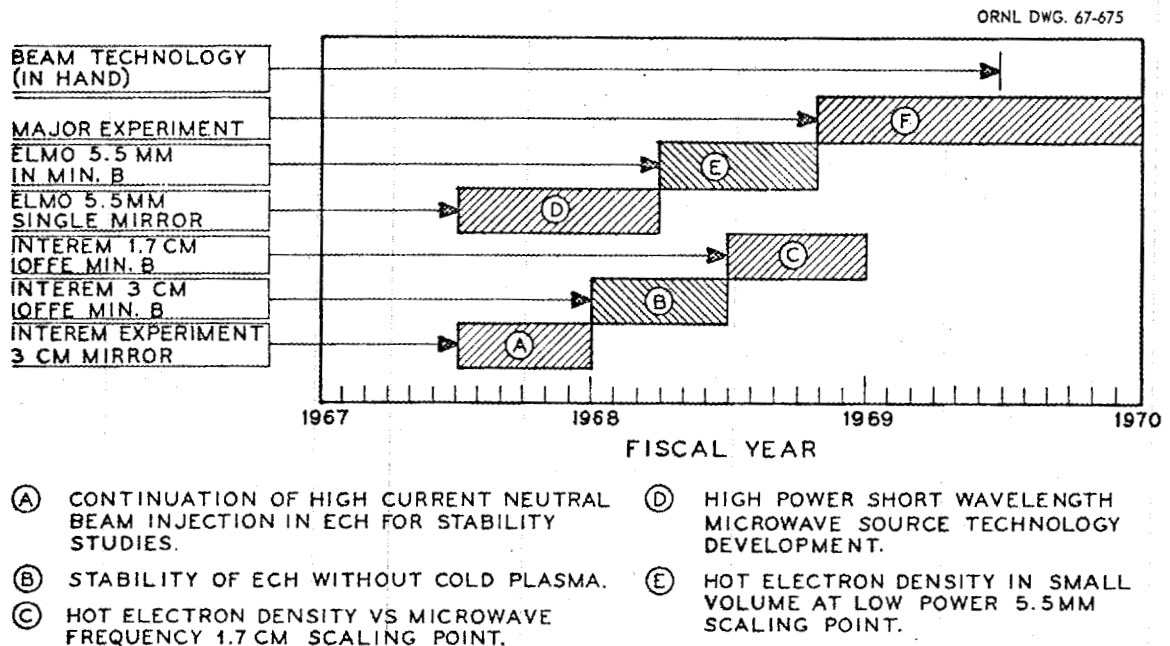


Fig. 2. Flow Diagram of Anticipated ORNL Program Culminating in a Major ECH Energetic Injection Experiment.

densities of $\sim 10^9$ ions/cm³. The central objective of these experiments is a study of the high-frequency instabilities associated with the fast-ion population. Verification of the Landau-damping constraint should be possible for electrostatic modes propagating (partially) along the magnetic field.

It is hoped that by fiscal year 1968 the quadrupole Ioffe-bar configuration mentioned above can be installed in the INTEREM facility (B). Studies with 3-cm microwave power will then be carried out to determine the behavior of steady-state electron-cyclotron-heated plasmas in such traps at low ambient gas pressure. If a stable plasma at low pressure can be produced in the Ioffe trap, design of a low-power 5.5-mm (20-kG) system can be initiated (E). During this same period, experiments will be performed to determine the power-scaling laws necessary to fix the design features of the full-scale experiment, using 1.7-cm and 5.5-mm microwave power (C and E). The 1.7-cm power should be available in the immediate future, and present plans call for development of the 5.5-mm source technology by the second quarter of fiscal year 1968 (D). Design and construction of the complete experiment could then follow in fiscal year 1969 (F). Although it is obvious that each succeeding step relies on success in the preceding step, we emphasize the important scientific and technological questions which remain to be answered: stability against high-frequency (especially flutelike) modes and an entire technology of electron-cyclotron heating in magnetic wells. Faced with these unanswered questions, any timetable can only be considered as indicative of the direction of the program.

STABILITY CONSIDERATIONS

In this section we shall summarize those aspects of plasma stability which are now thought to be relevant to the types of plasma systems under consideration. To begin with, then, it is necessary to review those features of the proposed systems having recognized implications for stability.

1. The confining magnetic field configuration will be a magnetic well, that is, will exhibit closed nested surfaces of constant $|\mathbf{B}|$, in which $|\mathbf{B}|$ increases outward from the center.
2. The target plasma, produced by electron-cyclotron-resonance heating, is expected to reach a density in excess of 10^{13} electrons/cm³ at a temperature of several thousand electron volts, with an equal density of ions at less than a hundred electron volts.
3. The injected neutral atoms, and the resulting trapped ions, will have a distribution of energies centered about 10 to 20 keV. Present beam technology permits distributions with $\Delta E/\bar{E} \sim 50\%$ (FWHM), and broader distributions may be anticipated in the future.
4. The plasma volume will be around 1 to 4 liters: $R_p > (5 \text{ to } 10)\rho_i$, $L_p > (10 \text{ to } 20)\rho_i$, where ρ_i is the 20-keV ion gyroradius.

The first of these considerations, choice of the magnetic well configuration, may be expected to stabilize most low-frequency instabilities, provided the well depth is chosen suitably. For example, the following theoretical criteria are available:

1. interchange stable if

$$\frac{\Delta B}{B} > \beta \text{ (ref. 1) ,}$$

2. universal modes stable if

$$\frac{\Delta B}{B} > \frac{1}{6} \frac{T_e}{T_e + T_i} \text{ (refs. 2, 3) ,}$$

3. long-wavelength drift-cyclotron stable if

$$\frac{\Delta B}{B} > \frac{1}{2} \frac{T_i}{T_i + T_e} \text{ (refs. 4, 5) .}$$

(This last criterion must be considered as only a provisional result; this mode is the object of a vigorous current research effort.) Although other specific modes have not been analyzed in search of similar "well-depth" criteria, it seems likely that most electrostatic modes with frequencies much less than ion gyrofrequency should be stabilized in practicable magnetic wells.

Instabilities Driven by Lack of Thermalization

Because an open-ended configuration has been chosen, we must anticipate those instabilities associated with inevitable departures of the plasma from thermal equilibrium as well as with the anisotropic ion distribution created by injection. In the following we discuss only the stabilization techniques which may eliminate the known high-frequency velocity-space instabilities.

Harris⁶ and Low-Density Loss-Cone⁷ Modes. — These growing waves propagate at angles of less than 90° with respect to the magnetic field. The associated axial electric field can lead to strong (electron) Landau damping provided the electron temperature is sufficiently high. We estimate the required temperature to be roughly

$$T_e \sim \frac{m}{M} \left(\frac{n L_p}{2\pi \rho_i} \right)^2 T_i$$

for $\omega \approx n\omega_{ci}$. Here L_p is the plasma length and m/M is the ratio of electron to ion mass. For example, if $L_p \sim 20\rho_i$ and $T_e \sim T_i$, harmonics up to $n \sim 10$ may be stabilized.

¹J. B. Taylor and R. J. Hastie, *Phys. Fluids* 8, 323 (1965).

²T. K. Fowler and G. E. Guest, p. 383 in *Plasma Physics and Controlled Nuclear Fusion Research*, vol. I (CN 21/99), IAEA, Vienna, 1966.

³J. D. Jukes, p. 643 in *Plasma Physics and Controlled Nuclear Fusion Research*, vol. I (CN 21/39), IAEA, Vienna, 1966.

⁴N. A. Krall and T. K. Fowler, GA-7393 (1966).

⁵W. M. Farr, Ph.D. thesis, University of Michigan, 1966.

⁶E. G. Harris, *J. Nucl. Energy C2*, 138 (1961).

⁷G. E. Guest and R. A. Dory, *Phys. Fluids* 8, 1853 (1965).

High-Density Loss-Cone⁸ Modes. — These growing waves have been predicted to be convectively unstable, and preliminary estimates have found their reflection at plasma extremities to be weak. On this basis they are not expected to grow to observable amplitudes in plasmas of length less than a critical value $\sim 100\rho_i$.

Flutelike High-Frequency Electrostatic Modes⁹. — We have already mentioned one example of this class of instabilities, the drift-cyclotron mode, which may be driven solely by the diamagnetic current. Other examples are caused by sharply peaked ion energy distributions, especially when a less energetic group of ions is also present in the plasma. This last circumstance is anticipated in the present program and may lead to unstable oscillations near the ion gyrofrequency. An intensive study of this class of instabilities is presently under way in an effort to assess realistic threshold conditions and growth rates.

Mirror Instabilities¹⁰. — These modes have been tentatively identified in electron-cyclotron plasmas¹¹ when the electron-temperature anisotropy and the plasma pressure were increased to relatively high values. By suitable choice of heating-zone location it should be possible to retain sufficient isotropy to prevent these instabilities.

Conclusions

In brief, we hope to obtain low-frequency stability from the magnetic well, relying on short length and Landau damping to stabilize high-frequency waves propagating partially along the magnetic field. The flutelike high-frequency modes may be stabilized by short-circuit effects (using conducting end walls), but these remain a serious unanswered question.

FUNDING

To prosecute the program of injection into the electron-cyclotron plasma, we build on what we have: the INTEREM facility with services already laid on, to which Ioffe bars will be added in fiscal year 1968 (existing generators capable of the required 8 MW, existing neutral-beam technology, and existing instrumentation). Accordingly, the greater part of the hardware cost for the fiscal year 1967, 1968, and 1969 programs shown in Fig. 2 can be absorbed into the regular operating budget of the Dandl group. The engineering and technician staffs are sufficient, but two physicists are needed. The big expense will not come until late fiscal year 1969 or 1970, so a summary of the cost would be as follows:

⁸R. F. Post and M. N. Rosenbluth, *Phys. Fluids* 9, 730 (1966).

⁹R. A. Dory, G. E. Guest, and E. G. Harris, *Phys. Rev. Letters* 14, 131 (1965); L. S. Hall, W. Heckrotte, and T. Kammash, *Phys. Rev.* 139, A1117 (1965).

¹⁰R. F. Post, *Nuclear Fusion*, 1962 Supplement, Part 1 99 (1962).

¹¹W. B. Ard, R. A. Dandl, and R. F. Stetson, *Phys. Fluids* 9, 1498 (1966).

Fiscal Year	Budget	Remarks
1967	\$625,000	
1968	\$765,000	Add 2 physicists. Install Ioffe bars. Normal 3% escalation.
1969	\$990,000	Escalation. Design and beginning fabrication on major facility.
1970	\$2,600,000	Completion of major facility. \$1.5 million for 5.5-mm microwave equipment, 100 kW.

This proposed funding replaces the B-budget item for \$1.5 million that was submitted for fiscal year 1968. The above figures will appear in our budget request for fiscal year 1969.

Appendix

TRAPPING OF 20-keV NEUTRAL ATOMS IN A TARGET PLASMA

The following calculation attempts to determine the average density of 20-keV protons resulting from the injection of a high-current 20-keV atomic neutral beam (the current being of the order of 1 A) into a dense (3×10^{13}) electron-cyclotron plasma (ECP) in magnetic mirror containment. The ECP is assumed to have a size sufficient to provide a thermal neutral shielding distance of at least five mean free paths for ionization of H_2^0 to H_2^+ .

The usual rate equation for the buildup of hot-ion density, n_i , is

$$\frac{dn_i}{dt} = j_1 - j_2 - j_3, \quad (1)$$

where

j_1 = average current of energetic ions trapped in a unit volume,

j_2 = average current of energetic ions charge transferring out of a unit volume,

j_3 = average current of energetic ions Coulomb scatter-lost out of a unit volume.

The calculation of j_1 is most conveniently accomplished by averaging the total current of hot ions over the volume filled by the hot ions. However, j_1 is calculated by first calculating j_r , where j_r is the trapped hot-ion current per unit volume at the radius r . The differential volume $dV = 2\pi r dr R$ is filled with hot ions from a trapping length $dL = 2 dr$. The factor 2 results from the precession of small orbits around the annulus formed by the assumed differential volume (see Fig. A1).

$$j_r = \frac{dL I_0}{dV \lambda} = \frac{2 dr I_0}{2\pi r dr R \lambda} = \frac{I_0}{\pi r R \lambda}$$

Note that since $j_r \propto 1/r$, the peak hot-plasma density would be expected to be at the center of the plasma.

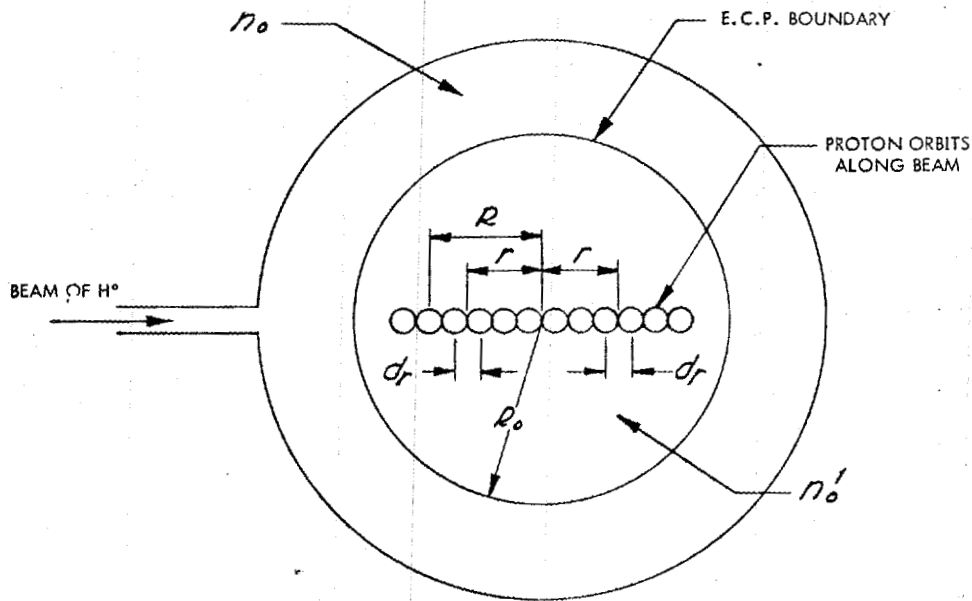


Fig. A1. Diagrammatic Cross Section of the Plasma.

The average energetic injection current

$$j_1 = \frac{1}{\pi R^3} \int j_r dV \quad (\text{assume cylindrical plasma } \dots Z = \pm R/2),$$

$$j_1 = \frac{1}{\pi R^3} \int_0^{2\pi} \int_0^R \int_{-R/2}^{+R/2} \frac{I_0 r d\theta dr dZ}{\pi r R \lambda} = \frac{2I_0}{\pi R^2 \lambda}.$$

The trapping of energetic neutrals in the case considered involves two dominant processes: trapping by ionization on hot electrons, the mean free path of which is λ_{ie} , and trapping by charge transfer to cold ions, the mean free path of which is λ_{cx} ;

$$\lambda_{ie} = \frac{1}{n_e \sigma_{ie} v_e / v_0}, \quad \lambda_{cx} = \frac{1}{n_e \sigma_{cx}}.$$

We assume that at all times $n_e = n_+$.

Examination of the cross sections for 20-keV hydrogen atoms shows λ_{cx} to be much the smaller and therefore the more dominant term, that is,¹

$$\lambda = \lambda_{cx},$$

¹J. R. McNally, Jr., private communication.

and

$$j_1 = \frac{2I_0 n_e \sigma_{cx}}{\pi R^2}, \quad (2)$$

$$j_2 = n_i n'_0 \sigma_{cx} v_i, \quad (3)$$

and

$$j_3 = \frac{n_i}{\tau_s}. \quad (4)$$

Substituting (2), (3), and (4) into (1):

$$\begin{aligned} \frac{dn_i}{dt} &= \frac{2I_0 n_e \sigma_{cx}}{\pi R^2} - n_i n'_0 \sigma_{cx} v_i - \frac{n_i}{\tau_s} \\ &= 0 \text{ in steady state,} \end{aligned}$$

and

$$\frac{2I_0 n_e \sigma_{cx}}{\pi R^2} = n_i n'_0 \sigma_{cx} v_i + \frac{n_i}{\tau_s}. \quad (5)$$

The neutral density in the center of the plasmas changes as

$$\frac{dn'_0}{dt} = i_1 - i_2 + i_3 + i_4 + i_5 - i_6, \quad (6)$$

where i_1 is the unit-volume current gain of slow neutrals made by charge transfer from energetic neutrals to cold ions, i_2 is the unit-volume current loss of slow neutrals by charge transfer to hot protons, i_3 is the unit-volume current gain of slow neutrals from outside the plasma due to wall reflux of slow atomic neutrals coming out of the plasma, i_4 is the unit-volume current gain of slow neutrals from outside the plasma due to wall reflux of energetic protons lost by charge exchange, i_5 is the unit-volume current gain of slow neutrals from outside the plasma due to the neutral gas input I_{Bg} (of course, this flux should be made as small as possible), and i_6 is the unit-volume current loss of slow neutrals due to their drift to the cavity walls:

$$i_1 = \frac{2I_0 R_0 n_e \sigma_{cx}}{V}, \quad (7)$$

$$i_2 = n_i n'_0 \sigma_{cx} v_i, \quad (8)$$

$$i_3 = \frac{2I_0 R_0 n_e \sigma_{cx}}{2KV}, \quad (9)$$

$$i_4 = \frac{V_H n_i n'_0 \sigma_{cx} v_i}{2KV}, \quad (10)$$

$$i_5 = \frac{I_{Bg}}{2KV} \quad (11)$$

$$i_6 = \frac{n'_0 v_f A}{4V} \quad (12)$$

Notice that in i_1 through i_6 the pessimistic assumption is made that no atomic neutrals (other than that fraction of energetic beam trapped) are ionized by the electron-cyclotron plasma. However, the complete ionization of thermal H_2^0 to H_2^+ is assumed to take place in the first few millimeters of ECP, and i_3 , i_4 , and i_5 result from molecular hydrogen entering the surface of the ECP.

The factor 2 in the denominator of i_3 , i_4 , and i_5 results in the consideration that H_2^0 is first ionized to H_2^+ , so only one-half the neutral atoms enter the plasma. The factor $1/K$ arises from the fraction of H_2^+ dissociatively ionized after excitation (Franck-Condon process).² It also includes the favorable effect of plasma pumping of molecular ions before dissociative ionization.

Substituting (7), (8), (9), (10), (11), and (12) into (6) and solving for n'_0 in the steady state,

$$n'_0 = \frac{2I_0 R_0 n_e \sigma_{cx} + (1/2K)(2I_0 R_0 n_e \sigma_{cx} + I_{Bg})}{(v_f A/4) + V n_i \sigma_{cx} v_i - (1/2K)(V_4 n_i \sigma_{cx} v_i)} \quad (13)$$

In order to simplify the numerical consideration of the previous expressions, the following assumptions and parameters are incorporated:

$$V_H = V = \pi R^3, \quad A = 4\pi R^2, \quad R_0 = R = 10 \text{ cm},$$

$$\sigma_{cx} = 6 \times 10^{-16}, \quad n_e = 3 \times 10^{13}, \quad K = 3.$$

Also, I_0 is expressed in amperes and I_{Bg} is expressed in terms of cavity pressure P_0 (torrs) outside the electron-cyclotron plasma, without energetic injection. Since $I_{Bg} = n_0 v_0 A/4$ and since $n_0 = P_0 \cdot 3.2 \times 10^{16}$, then $I_{Bg} = 1.9 \times 10^{24} P_0$.

Incorporating these factors into (13) gives

$$n'_0 = \frac{1.6 \times 10^{30} (I_0 + P_0 \cdot 1.3 \times 10^5)}{v_i (n_i + 3 \times 10^{12})} \quad (14)$$

Then substituting this relationship for n'_0 into (5) (τ_s calculated to be 1.5×10^{-2} sec for 20-keV protons in 3×10^{13} density plasma in a 3:1 mirror³):

$$n_i = 10^{12} [\sqrt{(2.05 I_0 + 9.35 \times 10^5 P_0 + 1.5)^2 + 30.9 I_0} - (2.05 I_0 + 9.35 \times 10^5 P_0 + 1.5)].$$

²R. J. Mackin and D. J. Rose, private communication.

³T. K. Fowler, *J. Nucl. Energy: Pt. C* **6**, 513-14 (1964).

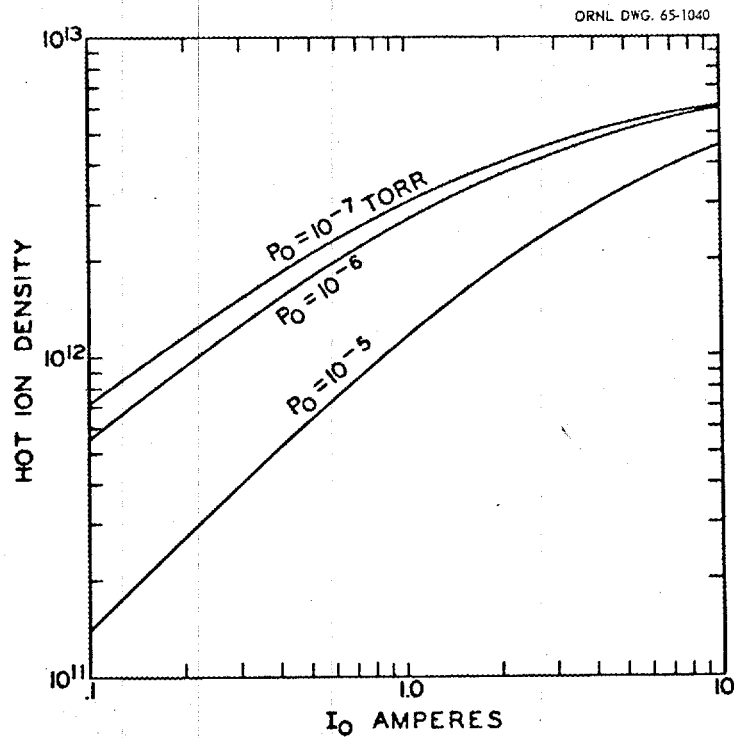


Fig. A2. Hot-Ion Density as a Function of 20-keV Neutral Injection Current.

Hot-ion density vs energetic (20 keV) neutral injection current is plotted in Fig. A2. The parameter for these curves is neutral pressure P_0 , ranging from 10^{-5} to 10^{-7} . Pressures in the region of 10^{-6} should be realizable outside electron-cyclotron plasmas, and beam currents in the neighborhood of $\frac{1}{2}$ A should be realizable with the few constraints imposed on them by this system. The 10^{-6} curve in Fig. A2 then indicates an average 20-keV proton density of 1.7×10^{12} . Since no advantage has been taken of the reduction of neutral flux by electron-cyclotron plasma ionization of atomic neutrals, and since a somewhat pessimistic scattering-loss relationship was employed, the above densities seem plausible.

LIST OF SYMBOLS

- Z = hot-ion plasma length
 R_0 = radius of ECP
 R = radius of hot-ion plasma
 n_0 = thermal neutral density outside plasma
 n'_0 = neutral density inside plasma
 n_i = hot-ion density/cc
 n_e = hot-electron density = $n_i + n_{i\text{cold}}$
 σ_i = ionization cross section for hot electrons on energetic neutral atoms ($\cong 6 \times 10^{-19}$) RB-71
 $\sigma_{01} = 2 \times 10^{-16}$ RB-34
 σ_{cx} = charge transfer cross section for 20-keV protons on neutral atomic hydrogen ($\cong 6 \times 10^{-16}$) RB-38
 v_i = velocity of 20-keV H^0 or H^+ = 2×10^8
 v_0 = velocity of thermal hydrogen = 2×10^5
 v_f = Franck-Condon or slow ion velocity = 3×10^6
 V = volume of ECP
 V_H = volume of hot-ion plasma
 I_0 = current in part/sec of 20-keV H^0
 τ_s = Coulomb scattering time for 20-keV protons

6.0 TECHNOLOGY

A summary of the technology involved with the work at ORNL could be supplied if necessary. The reason for omitting it at this point was the assumption that the Ad Hoc Panel was now concerned with existing and "immediate generation" machines, and the ORNL technology is state-of-the-art rather than developmental with regard to these machines.

Future machines, of course, rest upon development and technological research before becoming feasible. While ORNL does have strong efforts in this area, particularly in superconductivity, magnetics, ion sources, beam production, and electron cyclotron heating, the machines ORNL presents in this text are mainly those resting upon attained technology.

7.0 ECONOMICS IN OPEN-ENDED GEOMETRIES

If collective interactions can be controlled in an open-ended device, the energetic particles will be lost by long range coulomb interactions, which gradually change the direction of motion of the contained particles until they enter the loss cone. A very important question then is whether or not a reactor can be made to produce net power in the face of this kind of loss. Recent papers by Fowler and Rankin¹ and by Sivukhin² are somewhat pessimistic and very pessimistic respectively, but for different reasons.

The question had been discussed earlier by Post³. He had decided that if losses due to instabilities can be ignored, the prospects of net power production in such a device are very good. Fowler and Rankin's results differ from Post's for two related reasons. Post had considered the effect of electrons in the plasma only by determining the rate of energy loss of the hot ions to them. Fowler and Rankin considered also the effect of this energy loss on the spectrum of the energy of the contained ions, and the effect of the ambipolar potential difference produced by the automatic regulation of the plasma potential to equate input and loss rates of the charged particles. This potential difference enhances the loss of ions. Their calculations predicted only a very small positive energy balance.

Sivukhin's pessimistic conclusion came about because of his assumption that the ion distribution is forced by the particle feed to be quasi-Maxwellian. Under this condition there is a tremendous throughput of relatively cold ions and the losses due to the cycling of these particles are very severe. Hopefully it will not be necessary to maintain such a distribution.

It is possible to reduce the losses due to ambipolar potentials by the following means. A magnetic field is divided into three regions by four co-linear magnetic mirrors. Each region is a reactor with energetic particle feed. The entire plasma is at a high positive potential and electrons are contained in the system by the potential difference in the outer mirror throats. The central trap then contains ions without ambipolar enhanced loss, and the efficiency of the overall system will lie between that calculated by Post and by Fowler and Rankin.

The charge neutrality required in the mirror throats can be obtained by cold ions held in a shallow potential well. The kinetic energy loss of the hot ions to them can be as low as about 2% of the total loss.

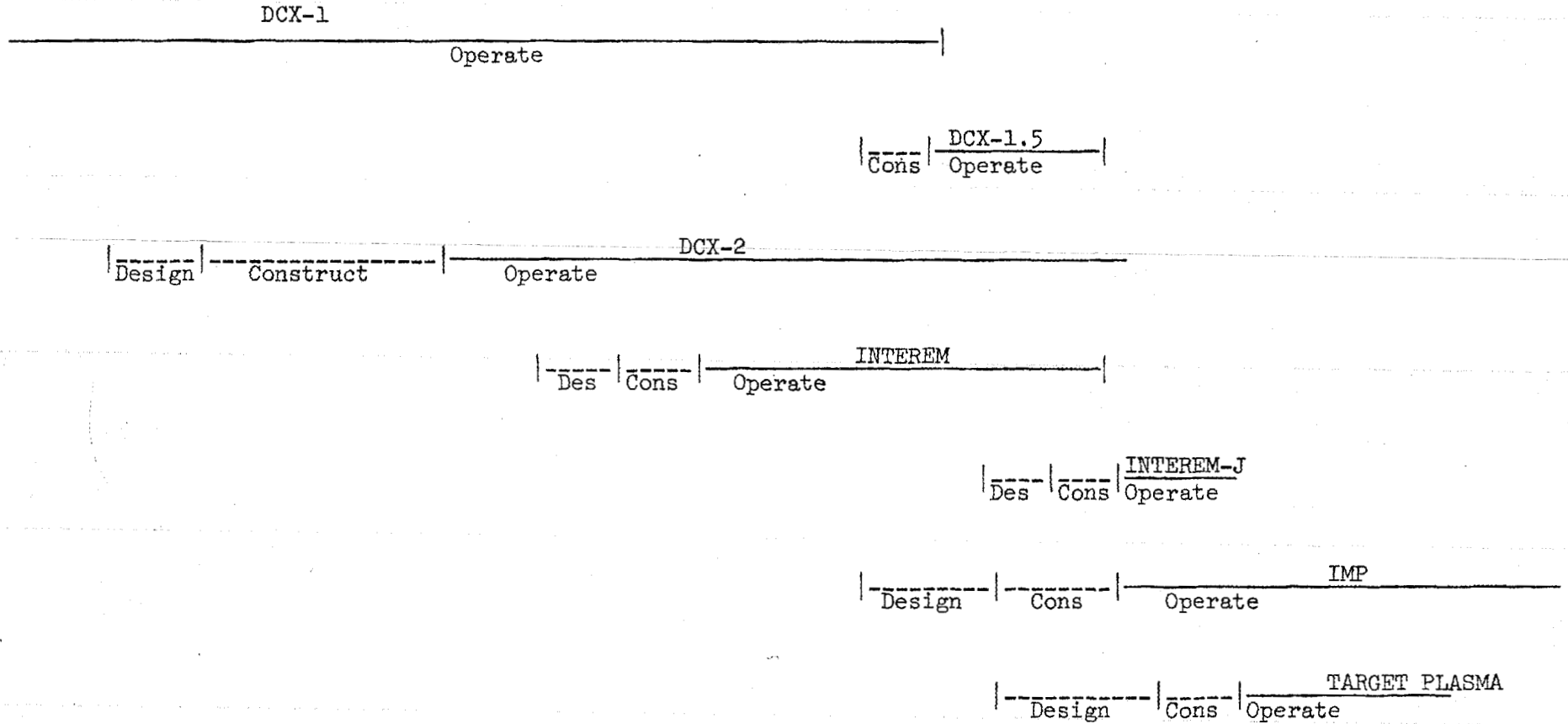
Thus the overall effect of the ambipolar potential can be greatly reduced. If the central trap, in which the axial potential variation is small, can be made large compared to the end regions, the average ion lifetime is increased. There is a corresponding increase in electron lifetime obtained by a slight increase in the potential of the plasma. Each electron is heated longer and the electron temperature rises toward the value assumed by Post. The energy balance for the device then will be the average of the values obtained by Post and by Fowler and Rankin, weighted by the ratios of the volumes in which these figures apply, to the total volume.

REFERENCES

1. Fowler T. K. and Rankin M. (1966) Plasma Physics (J. Nuc. Energy Part C) 8, 121.
2. Sivukhin D. V (1966) Plasma Physics (J. Nuc. Energy Part C) 8, 607.
3. Post R. F. (1962) Nuclear Fusion Supplement Part 1, 99.

CALENDAR YEAR TIME SCHEDULE OF ORNL INJECTION EXPERIMENTS

1958 1959 1960 1961 1962 1963 1964 1965 1966 1967 1968 1969 1970 1971 1972



8.2 CHART SUMMARIES OF PARAMETERS OF ORNL INJECTION EXPERIMENTS

Following are charts which outline the various ORNL parameters and results. The problem in making such charts is that it greatly over-simplifies and condenses the experiments and thus may be wrongly interpreted scientifically. On the other hand, because it does condense facts it is of use in summarizing pertinent information for ready reference. It is hoped that further references to the Chrestomathy, to publications, and to ORNL semiannual reports will give a broader perspective to these tables. Charts are given for technological, scientific, and administrative areas.

MACHINE NAME	MAGNETIC FIELD			VACUUM		TECHNOLOGICAL		ELECTRON CYC. HEATING			PLASMA VOLUME		STATUS
	SHAPE	(B ₀) STRENGTH	COIL TYPE	OPERATING PRESSURE	BEAM ENERGY	INJECTION METHOD BEAM INTENSITY	TRAPPING MECHANISM	PREQ	RES FIELD	POWER	RADIUS	AXIS	
DCX-1a	2:1 Mirror	10 kg	water cooled	10 ⁻⁷ torr	600 keV H ₂ ⁺	15 ma	C Arc dissociation	--	--	--	11"	0-20"	TERMINATED
b	2:1 Mirror	10 kg	water cooled	10 ⁻⁹ torr	600 keV H ₂ ⁺	15 ma	Gas dissociation	28 kmc	9.8 kg	50 w	11"	0-20"	TERMINATED
c	2:1 Mirror	"	"	"	"	1 ma	Lorentz dissociation	"	"	"	11"	"	TERMINATED
DCX-1.5	2:1 Mirror	≤ 14 kg	water cooled	2x10 ⁻⁹ torr	15 keV H ⁰	44 ma	Lorentz ionization	35 kmc (not tried)	12.4 kg	≤ 2 kw	8"	0-20"	OPERATE UNTIL DEC.
DCX-2	3:1 Mirror	13 kg	water cooled	5x10 ⁻⁸ torr	540 keV H ₂ ⁺	70 ma	GAS ARC.	--	--	--			OPERATE
INTEREM	2:1 Mirror	2.7 kg	water cooled	1x10 ⁻⁵	20 keV H ⁰	20 ma	charge exchange	10.6 kmc	3 kg	40 kw (central)			TERMINATED
				2x10 ⁻⁶	20 keV H ⁰	200 ma	trapping	10.6 kmc	3 kg	25 kw (end fed)			OPERATE
INTEREM + (J BARS)	2:1 Axial Mirror 1.5:1 Radial Mirror	2.7 kg	water cooled	variable	(possibility awaits calc.)			10.6 kmc	3 kg	40 kw (central)			CONSTRUCTION (OPERATE 10/67)
IMP a	2:1 Axial Mirror	20 kg	supercond.	< 10 ⁻⁹	20 keV H ⁰	(100 ma)	Lorentz ionization	5 ma	19 kg	100 w	10 cm		CONSTRUCTION
b	1.3:1 Radial Mirror	"	"	variable	none		cascade; cold plasma	5 ma	19 kg	5 kw	10 cm		(OPERATE 2/68)
c	"	"	"	variable	none		none	5 ma	19 kg	5 kw	10 cm		

SCIENTIFIC

MACHINE NAME	MACROSTABILITY		MICROSTABILITY		DENSITY	ENERGY	LIFETIME	DENSITY LIMIT	CAUSE OF LIMIT TO DENSITY
	FLUTE STABILITY THRESHOLD	CURE OF LOW FREQ. INSTAB.	MICROINSTABILITY NAME	CURE OR MODIFICATION					
DCX-1a	NOT OBSERVED	ARC PLASMA	NOT IDENTIFIED		5x10 ⁹	300 keV	14 ms	5x10 ⁹	volume expansion of plasma
b	(> 5x10 ⁸)	FINITE ORBIT	NEGATIVE MASS	ΔE, Δr, fieldgrad.	2x10 ⁸	300 keV	180 sec	2x10 ⁸	negative mass instability
c	(> 5x10 ⁸)	"	HARRIS-LIKE MODES	ECH (CURED)	2x10 ⁸	"	"	"	"
DCX-1.5	observed to limit at 3x10 ⁷	"line tying"	"θ-type" "Z-type"	High B ₀ , ΔE ECH (?)	4x10 ⁸	15 keV	160 ms	not limited	charge exchange
DCX-2	NOT OBSERVED	variable Precession freq. or Cold Plasma	1) Burt Harris Mode 2) Harris Mode 3) Ion-Ion Multigroup		5x10 ⁹	700 keV	150 ms	not limited	charge exchange
INTEREM	"	Cold Plasma Cold Plasma	None Observed None Observed	(T _e ?) (cold Plasma ?)	9.6x10 ⁸ (ions) 10 ¹¹ (electrons)	20 keV 100 keV	200 μs	not limited	charge exchange power limited
INTEREM+J	(not expected) for n _c /n _H >> 1	min-B	(to test)		?	?	?	?	?
IMP	(not expected)	min-B	1) Harris-like Modes 2) Ion-Ion Modes ECH ?	ECH T _e , ΔE	(10 ¹⁰) ions (10 ¹¹) ions (10 ¹³) electrons	20 keV 20 keV	(200 ms) (200 ms)	? ? ?	? ? ?

ADMINISTRATIVE

MACHINE NAME	MANPOWER	COST OPERATE 1000's	COST OF CONSTRUCTION 1000's
DCX-1	3 Phys 3 Eng 2 Tech	\$380/yr	?
DCX-1.5	3 Phys 2 Tech 3 Eng	\$420/yr	\$20 (ion source)
DCX-2	4 Phys 4 Eng 3 Tech	\$800/yr	\$2000 (1961)
INTEREM	2 Phys 2 Eng 2 Tech	\$400/yr	from operating funds
INTEREM + J Bars	"	\$400/yr	\$20 for bars
IMP	3 Phys 3 Eng 2 Tech	\$480/yr	\$250 from Thermonuclear Division (ORNL)

8.3 ENGINEERING ASPECTS OF THE IMP MAGNET SYSTEM

8.3.1 Introduction

As described in earlier sections, the IMP facility will be part of the Target Plasma Program. It will use energetic neutral injection and trapping in electron cyclotron plasmas established at low ambient neutral pressures (of order 10^{-8} torr). The magnet system will be of the mirror-quadrupole type, with central field values up to 20 kilogauss, a nominal 2:1 axial mirror ratio, and closed modulus B contours up to 26 kilogauss (with $B_0 = 20$ kilogauss)¹.

The facility features superconducting magnets, which in principle offer greater access to the plasma region than would be possible with copper coils. In addition, the operation of the superconducting system rather than the 20 megawatt copper system previously considered² allows the use of this power by other experimental devices.

8.3.2 Design Criteria

To avoid magnet instabilities we have chosen to use stabilized multifilament superconducting wire. Since maximum current density is required for deep wells at large B_0 , the design criterion provides for operation very close to the limit of reversible stabilization (i.e., with the maximum superconductor-to-copper ratio which will still provide smooth controlled transitions into a resistive mode of operation). The need for high current density also implies that insulation and liquid helium spaces in the winding volume must be minimized subject to the constraint that cooling passages remain sufficiently open to allow free flow of helium gas bubbles.

¹A compensation ratio of 1.75 is required for a last closed contour of 26 kilogauss with $B_0 = 20$ kilogauss. (Compensation ratio is defined as the ratio of quadrupole current to that just required to null out the negative radial gradient of the mirror field 0.5 cm off axis in the median plane).

²Thermonuclear Div. Semiann. Progr. Rept. Oct. 31, 1966, ORNL-4063, pp. 29-35.

The mechanical system of IMP must restrain all electromagnetic and gravitational forces. In addition, it must maintain vacuum integrity and withstand fault condition overpressures of the liquid helium system. The extreme forces between coils require that all magnets and their associated mechanical structure must operate at 4.2 K, so that force bearing members are isothermal and need not be minimized for heat loads.

The magnet configuration utilizes mirror coils inside the Ioffe (quadrupole) coils to provide the necessary high radial mirror field gradient in the midplane (for Lorentz trapping). This configuration also offers the maximum plasma volume. After considering two coil and four coil (symmetric and near-symmetric) Ioffe coil systems, we have chosen a design which uses two symmetrical sets of two coils each (see Fig. 1). This coil arrangement facilitates winding and minimizes the coil winding material while maximizing the field contribution.

8.3.3 Present Design Status

Early calculations of the IMP magnet system indicated that current densities of 10^4 amperes/cm² would be required to generate the desired field shape. The maximum fields in the conductor windings were found to be 68 kilogauss in the mirror coils and 73 kilogauss in the Ioffe coils. However, after optimization procedures were applied, it was found possible to lower the current density to 8500 amperes/cm² for the same Ioffe field contribution. This reduction of current density also led to lower maximum field intensities in the magnet windings; i.e. 66 kilogauss in the mirrors and 67 kilogauss in the Ioffe coils.

Fig. 2 shows a conceptual layout of the mirror-quadrupole system in the liquid helium container. Though not indicated on the drawing, the coil cans (mirror and Ioffe) are porous to allow adequate helium ventilation through the superconducting winding volume. The ends of the helium containment vessel also serve as primary structural members. Each Ioffe coil will be bolted to the

thick end plates. The mirror coils will nestle inside the Ioffe coils and will be restrained from axial motion by tie-bars to the end plates. The coil cans will be fabricated from high strength aluminum alloy (7039 T-6). Each will be cut from a single piece of material to avoid low strength weldments. The liquid helium container including end plates will be fabricated from a weldable medium strength aluminum alloy (3083 H321).

The six access ports into the central plasma region, and this region itself, are lined with a variable temperature wall. Except during periods of outgassing or extreme high vacuum these walls will be maintained at approximately 77°K. The ports allow access for beam injection, beam dump, waveguides, and plasma probe instrumentation; and provide pumping conductance to the surrounding vacuum region (see Fig. 2).

The choice of a proper superconductor wire has been complicated by the limited state-of-the-art in understanding the detailed performance of superconductors. After considering the inter-related requirements of stabilizing material, superconducting material, helium ventilation space, insulation, and forces, we chose a conductor offered by Avco-Everett Research Laboratories. An order for 100,000 feet has been placed.

This conductor is shown in Fig. 3. The 15 superconducting strands are NbTi are imbedded in a matrix of high conductivity copper. Two-thirds of the conductor cross-section is stabilizing copper, the other third is NbTi. The short sample performance is 535 amperes at 75 kilogauss; the coil design current density indicates that a conductor current of 450 amperes or less will be required. A spiral wrap of H. T. Nomex* paper 0.005" thick by 0.080" wide provides turn-to-turn spacing for insulation and helium ventilation. A preliminary experiment indicated that

*Trademark of E. I. DuPont

the passage of helium bubbles is influenced very little by a gap of 0.005" or greater. However, with tighter spacing helium bubbles would be delayed in passage and accumulated, leading to a premature normal state transition. Decisive factors in our choice of this insulation were the evaluations of its performance at low temperatures by H. Brechna of SLAC³ and A. G. Prodell of BNL⁴. It appears to have better strength and creep properties than either 66 nylon or mylar. We feel that by covering 50% of the conductor surface it will be possible to avoid shorts in the coil.

A test of conductor and insulator performance in a magnet is planned for the very near future. The conductor will be used to wind two identical coils which will then be mounted in series-opposition (cusp configuration) with a horizontal axis. This coil set will be tested in a homogeneous 65 kilogauss external magnetic field of a solenoid with vertical axis. The test should simulate the actual field intensities, current densities, and forces in the full IMP magnets. It will also approximate the type of cooling environment to be found there.

Model studies of the best winding methods are in progress. These tests will lead to detailed techniques for winding, maintaining adequate wire tension, preventing "bowing" in the straight sections of the Ioffe coils, making interlayer transitions, splicing conductor, etc.

The cryogenic system, outlined in Fig. 4, will provide for cooldown and operation of the magnet. Those parts shown in the lower right section of the figure will be installed for preliminary experiments with only the mirror coils. Cooldown will be effected by passing liquid nitrogen through cooling lines attached to the end plates. Conduction through the helium exchange gas around the coils

³International Cryogenic Engineering Conference, April 9-13, 1967, Kyoto, Japan.

⁴Personal communication.

and the mechanical structure completes the cooldown. After satisfactory operation of the mirrors, the quadrupole set will be added along with the full cryogenic system as shown. Cooldown losses are expected to be ~ 300 liters of liquid helium. Thereafter, operating losses should be ~ 40 liters per day. Optimized input current leads will be used to avoid unnecessary lead losses. These leads will be detachable to further reduce heat leaks when the machine is not in operation. Rupture discs and an automatically operated gas blow-off stack will provide for the heavy gas loads which might occur upon a full normal state transition.

The IMP magnet electrical system is shown in Fig. 5. A solid state power supply will energize the series-connected mirror coils. One or more protective diodes across the supply avoids the possibility that the coil might damage the supply. Another diode, in series with a large resistor, provides for coil energy dumping in the event of a normal state transition. The use of a diode here eliminates resistor current during magnet charge-up. When a normal state transition is detected the switch to the power supply is opened, leaving the resistor as the only current path for the magnet current. The resistor is chosen as large as the coil insulation will reasonably allow, so that maximum energy is dissipated in the resistor rather than in the coil. We expect to use a resistor value of 0.2 to 1.0 ohms. The charging time of the mirror coil set could be as fast as 100 seconds (for a constant 10 volt charging potential).

One wishes to obtain an early indication of any normal state resistance in order to prevent, if possible, a full energy discharge and to automatically activate the energy dump circuitry if the full discharge cannot be avoided. For this purpose we will monitor the coil voltages with a difference amplifier in order to detect a resistance in either of the coils. A heater on the critical turn in the

coil will also be used, in a manner suggested by John Stekly of Avco⁵, to anticipate the critical current of the coil. Sensors will be built into the coil cans to monitor coil can temperature, critical turn temperature and voltage, and critical magnetic field intensities near the conductor.

The electrical system for the series-connected Ioffe coils is very similar to that for the mirror coils. Difference voltages will be monitored for each of the coil pairs. The energy stored in this system is much higher (more than 3 megajoules), so two energy dump resistors will be used for speedy discharge while holding the discharge voltages to 500 volts or less. The higher stored energy also dictates longer charging times. A minimum of 30 minutes would be expected. However, the final stages of charging would probably proceed much more slowly to prevent an unpredicted transition, so the actual charging times will probably be in the order of 45 minutes. The heater arrangement of Stekly will be employed in each coil of the Ioffe set, and the various sensors will be built into each coil can.

Persistent mode switches would be desirable to reduce helium losses during operation. However, these switches must be very reliable to avoid the possibility of coil damage if they failed to open during a transition. The development of an appropriate switch will proceed with the hope that it might be employed after experience has been obtained separately with the coil system and the switch.

Superconducting material is scheduled for delivery in July and August. Present plans are for operation of the mirror coil system in the fall of 1967 and operation of the mirror-quadrupole system in the spring of 1968.

The assistance of Dr. C. N. Whetstone of Air Reduction Company is gratefully appreciated.

⁵Z.J.J. Stekly, "The Performance of a Large MHD-Type Stable Superconducting Magnet", Avco Research Laboratories, Rept. AMP 215, Dec., 1966. (Presented at the International Conference on High Magnetic Fields, Grenoble, France, Sept. 12-14, 1966).

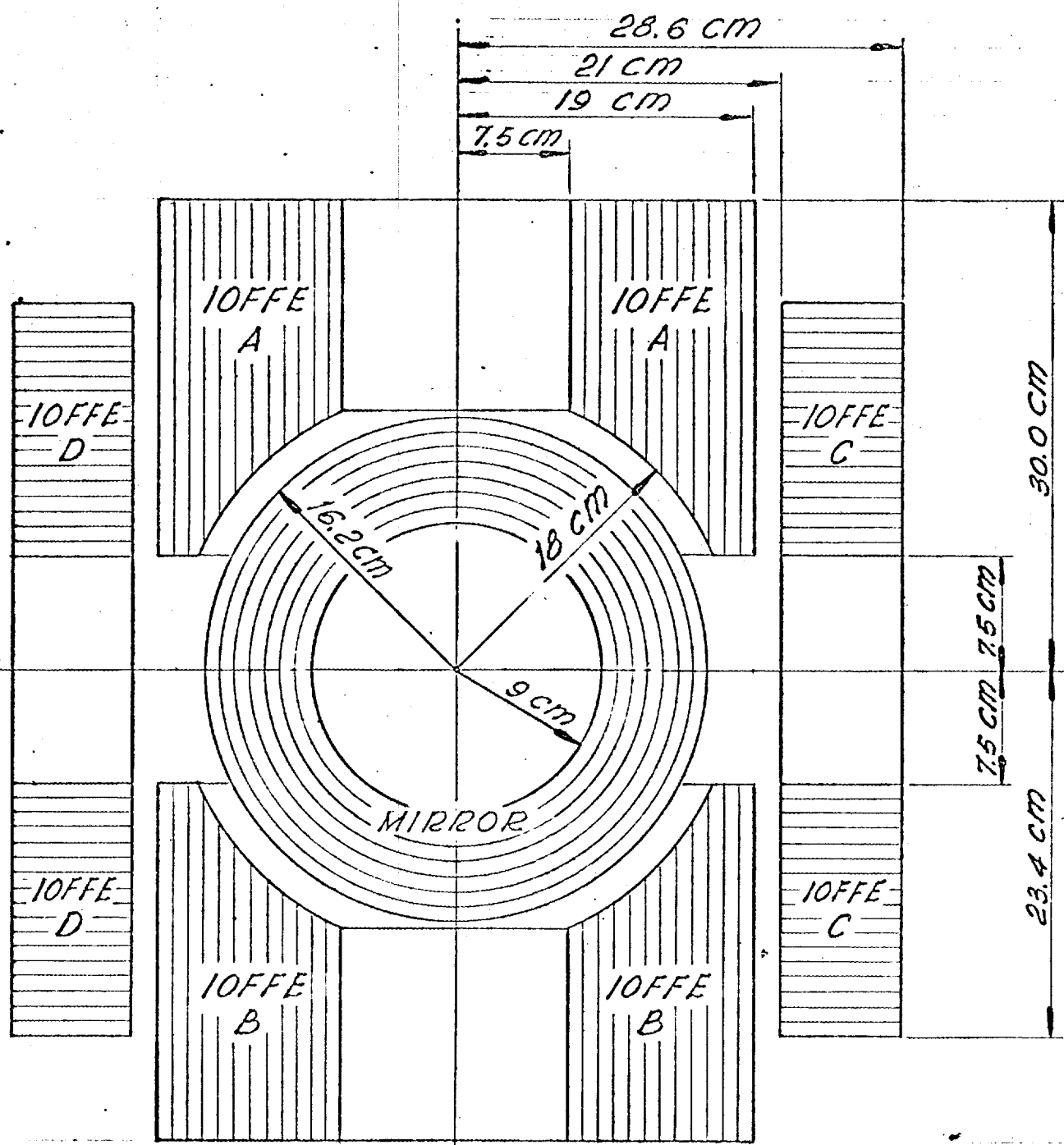
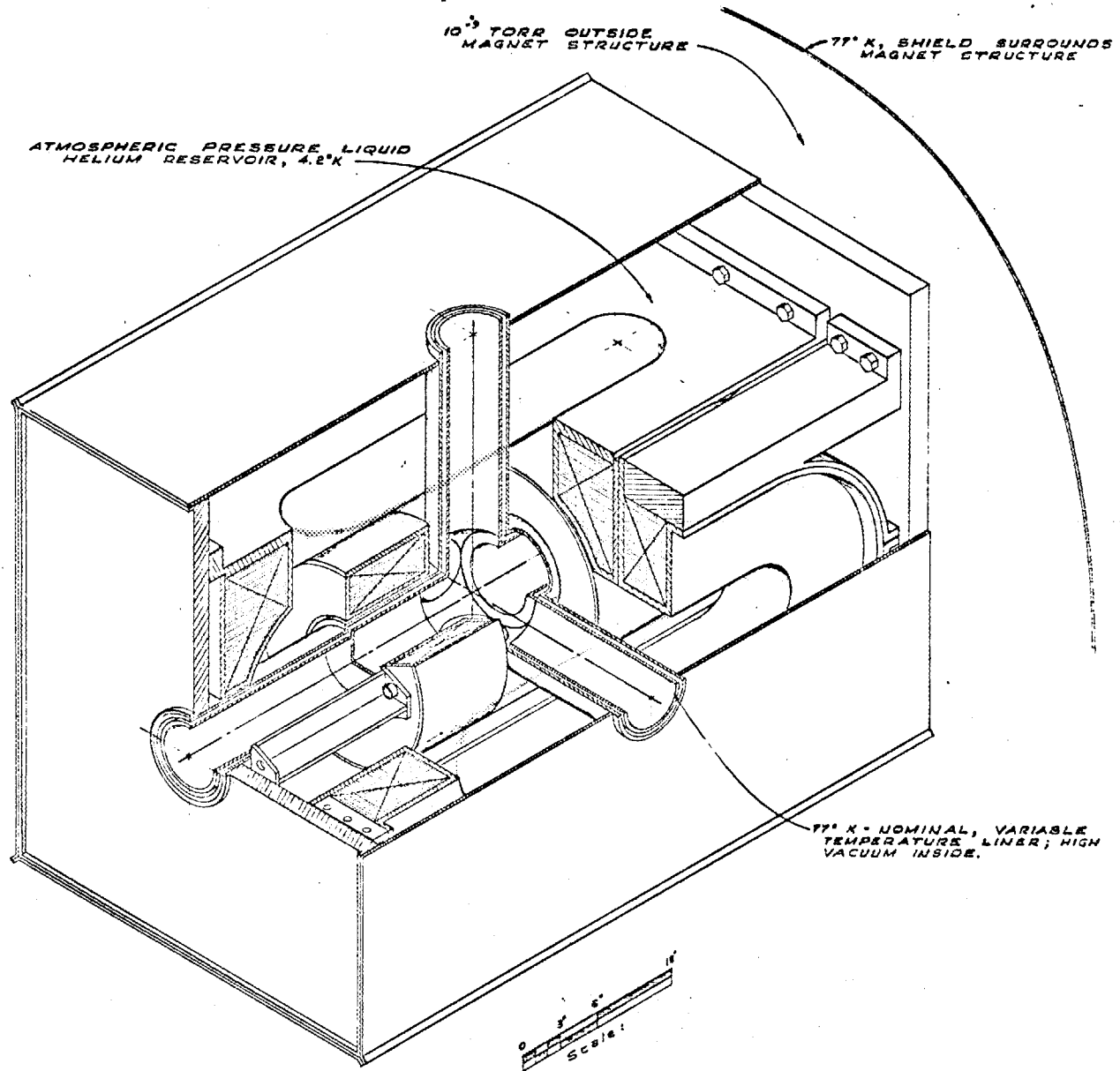


FIG. 1

MIDPLANE CUT SHOWING AN AXIAL
VIEW OF THE IMP COIL CONDUCTOR
CROSS SECTION.



75

FIG. 2

I. M. P.

CONCEPTUAL LAYOUT

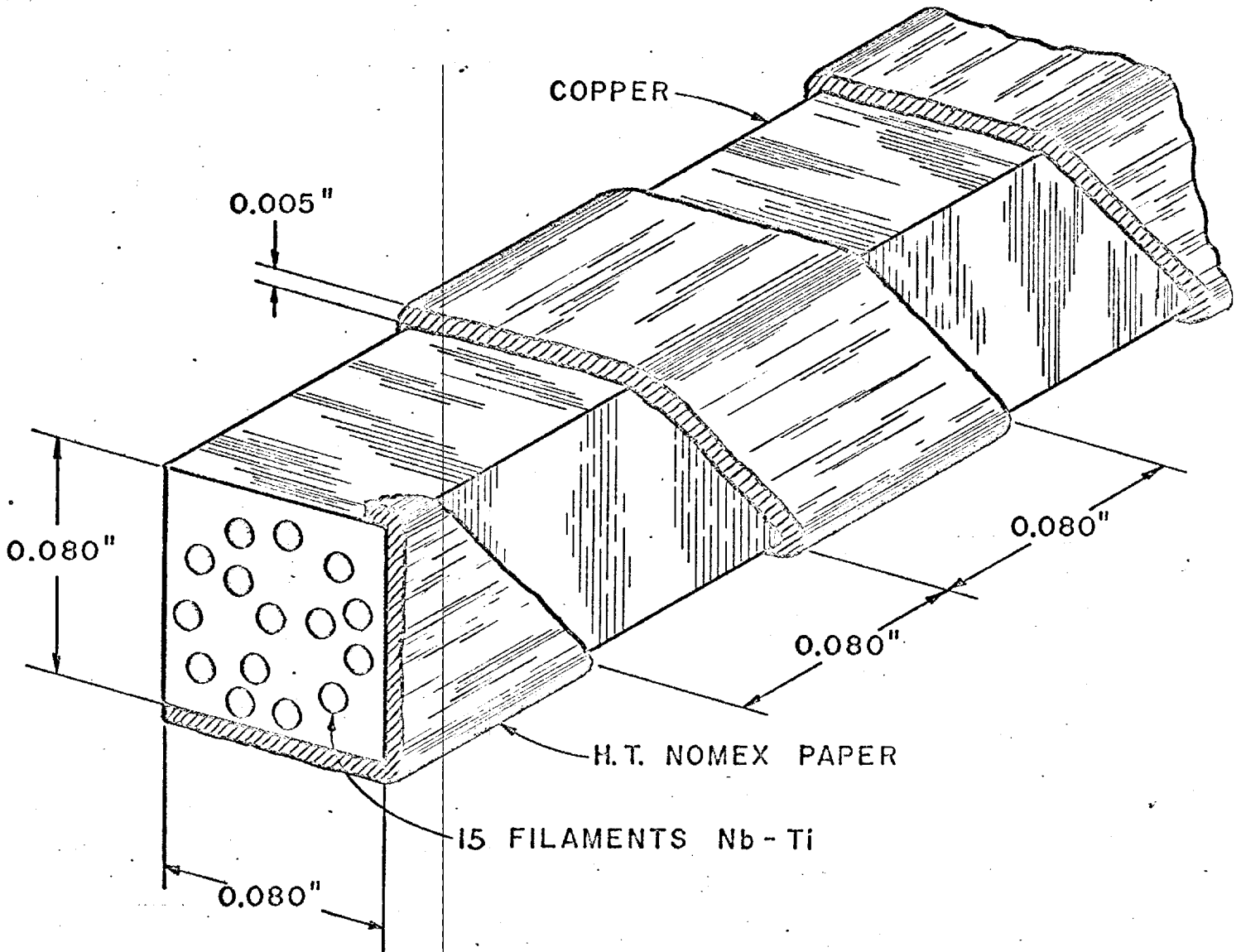


FIG. 3
I.M.P. SUPERCONDUCTOR

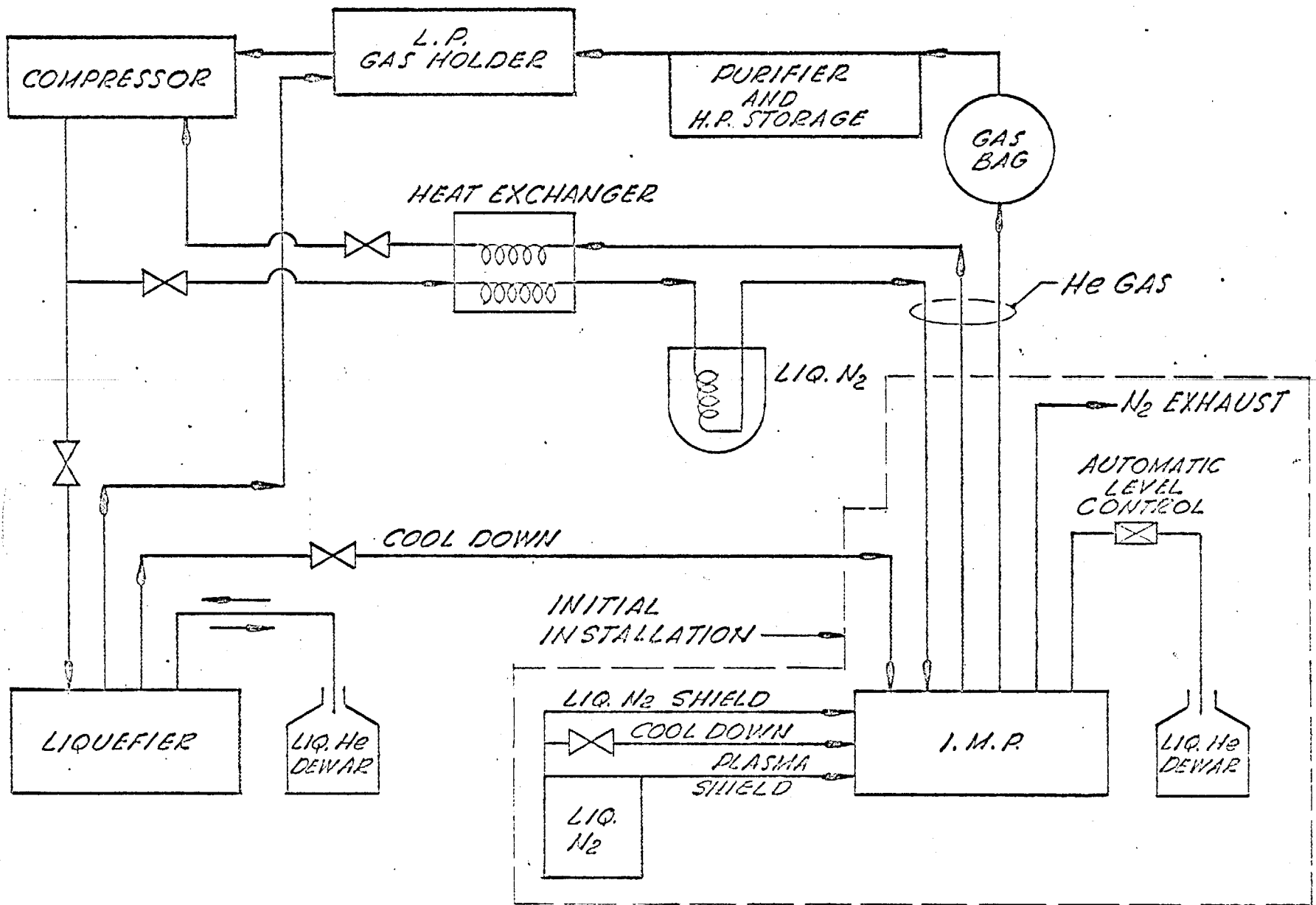


FIG. 4 I.M.P. CRYOGENIC SYSTEM

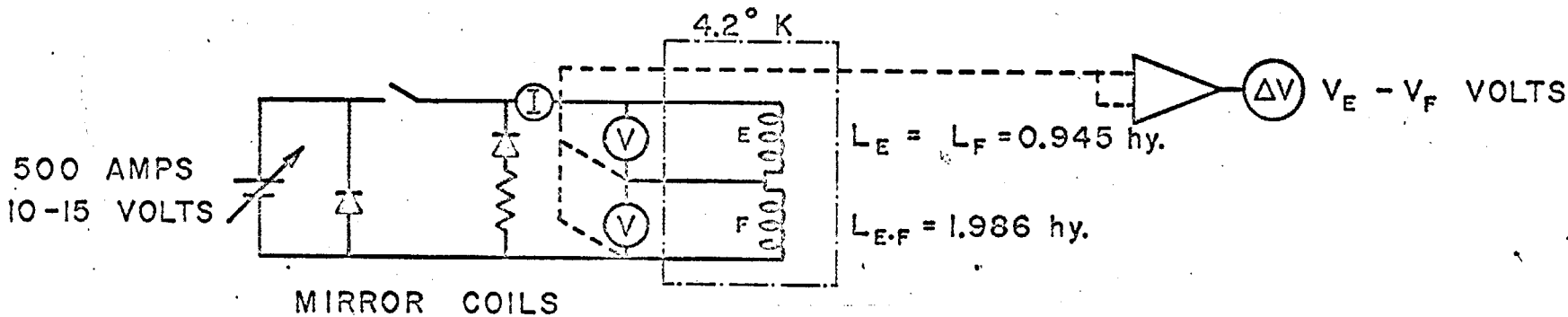
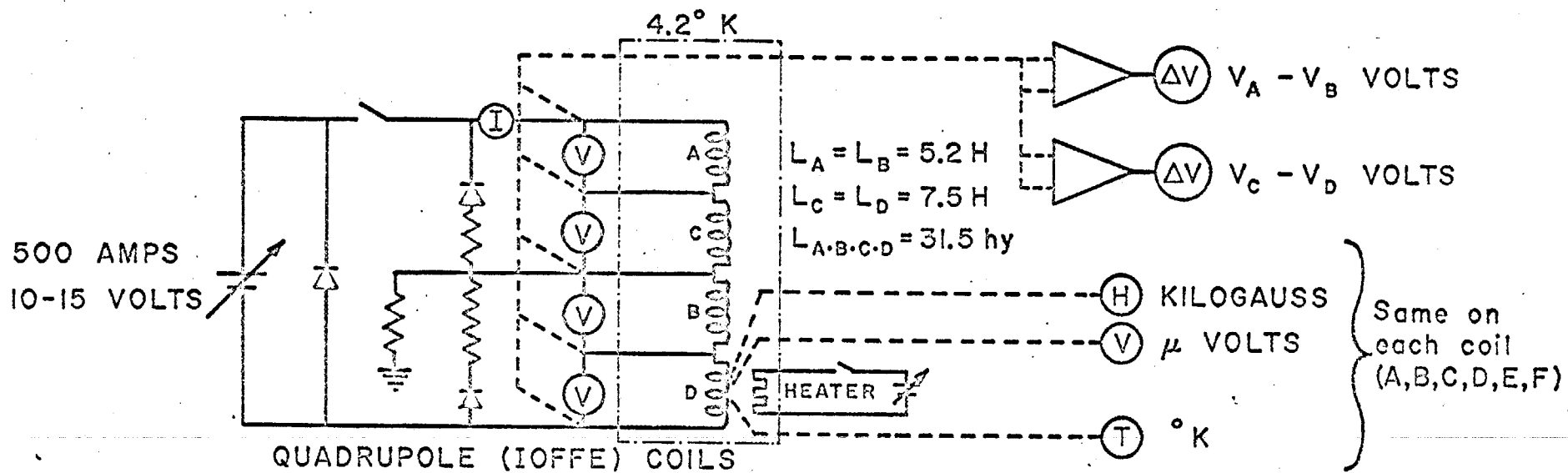
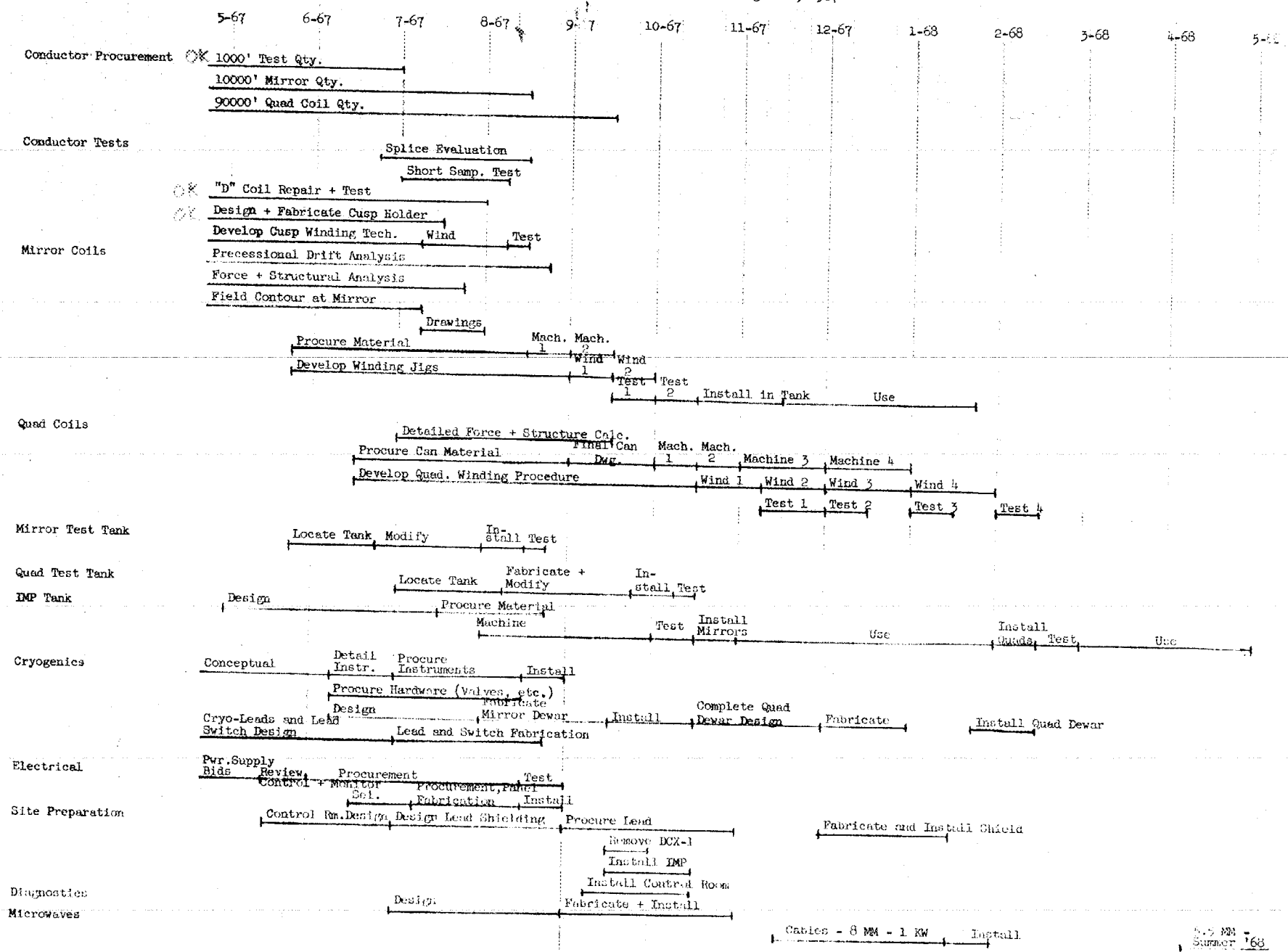


FIG. 5

I.M.P. ELECTRICAL SYSTEM

Kastner

IMP WORK SCHEDULE - August 1, 1967



IMP WORK SCHEDULE - JULY 1, 1967

